Developmental Biology
Neuroscience

Lineage-specific intersection of endothelin and GDNF signaling in enteric nervous system development

Reviewed Preprint
v2 • November 15, 2024
Revised by authors

Reviewed Preprint
v1 • April 29, 2024

Denise M Poltavski, Alexander T Cunha, Jaime Tan, Henry M Sucov, Takako Makita

Department of Regenerative Medicine and Cell Biology, Medical University of South Carolina, Charleston, USA

eLife Assessment

This study provides **valuable** insights into our understanding of the development of the enteric nervous system. The authors use genetically engineered mice to study the behavior of stem cells in organizing the enteric nervous system and the secreted signals that regulate these cells. The study rests on a degree of **incomplete** evidence since the characterization of some of the mouse resources is not complete in the current version.

https://doi.org/10.7554/eLife.96424.2.sa3

Abstract

Two major ligand-receptor signaling axes – endothelin Edn3 and its receptor Ednrb, and glial-derived neurotrophic factor (GDNF) and its receptor Ret – are required for migration of enteric nervous system (ENS) progenitors to the hindgut. Mutations in either component cause colonic aganglionosis, also called Hirschsprung disease. Here, we have used Wnt1Cre and Pax2Cre in mice to show that these driver lines label distinct ENS lineages during progenitor migration and in their terminal hindgut fates. Both Cre lines result in Hirschsprung disease when combined with conditional *Ednrb* or conditional *Ret* alleles. In vitro explant assays and analysis of lineage-labeled mutant embryos show that GDNF but not Edn3 is a migration cue for cells of both lineages. Instead, Edn3-Ednrb function is required in both for GDNF responsiveness albeit in different ways: by expanding the Ret^{+} population in the Pax2Cre lineage, and by supporting Ret function in Wnt1Cre-derived cells. Our results demonstrate that two distinct lineages of progenitors give rise to the ENS, and that these divergently utilize endothelin signaling to support migration to the hindgut.

Introduction

The enteric nervous system (ENS) is the largest division of the peripheral nervous system and harbors a complex circuitry. Approximately a half billion enteric neurons in human (and over a million in mice) distribute along the entire axis of the gastrointestinal tract to regulate a variety of

physiological functions (Furness, 2006). Colonic peristalsis that promotes defecation is controlled by several subtypes of enteric neurons that reside in the myenteric plexus that is located between the longitudinal and circular muscles of the gut. Colonic myenteric mechanosensory neurons are multiaxonal (Dogiel type II) neurons of which one axonal branch extends to the gut mucosa and synapses with mechanosensory (enterochromaffin) cells, while the opposite branches synapse on motor neurons or interneurons in neighboring myenteric ganglia. When mucosal enterochromaffin cells are stimulated by the presence of feces, mechanosensory endings are activated and then transmit signals through interneurons to activate or inhibit motor neurons, which generate contraction or relaxation of colonic circular muscle, resulting in peristalsis. This neural circuitry enables the ENS to sustain autonomous gut motility in the absence of central nervous system input.

The entirety of the ENS has been thought to arise exclusively from migratory neural crest cells. This conclusion was based primarily on avian intraspecies cell transplantation (Le Douarin, 1982) and dye labelling studies (Serbedzija et al., 1989), and subsequently supported by genetic labelling studies of the neural crest cell lineage in mice (Yamauchi et al., 1999, Kapur, 2000, Yu et al., 2024). Enteric neural crest cells arise from the vagal region of the hindbrain and cervical spinal cord, migrate first to the foregut, and then continue to migrate along and colonize the entire length of the gut. Once in the gut, these organize into intrinsic ganglia, including the colonic myenteric plexus that has primary control of gut motility. A distinct sacral neural crest cell population colonizes the hindgut, migrating from the distal end of hindgut in a cranial direction (Anderson RB, 2000). The majority of sacral neural crest cells constitute the pelvic ganglia that are located on the rectal wall and project rostrally along the colon to supply sympathetic and parasympathetic control of gut physiology, but not including colonic peristalsis (Keast, 1995). Neural crest clearly contributes substantially to the ENS, and while past studies could not formally exclude a contribution from other sources, there has also been no experimental observation that would invoke the involvement of any other developmental origin.

Defective caudal migration of enteric progenitors results in aganglionosis in the terminal bowel. This has no consequence in fetal life while gut motility is suppressed, but after birth, when fecal progression through the hindgut requires a functional ENS circuitry, absence of adequate ENS function leads to congenital gut motility disorders, characterized by the inability to defecate and involuntary fecal retention. In such cases, the hindgut expands to accommodate the accumulating material, accounting for one name of this condition as congenital megacolon. A synonymous term for this pathology is Hirschsprung disease.

Hirschsprung disease is an inherited or sporadic condition in humans, and is associated with mutations in genes encoding two pairs of extracellular ligand/receptor signaling molecules: the endothelin ligand EDN3 and its G-protein coupled receptor EDNRB, and the receptor tyrosine kinase RET and its ligand GDNF (Parisi and Kapur, 2000). Mice that carry mutations in these genes lack intrinsic ganglia in the distal colon and therefore phenocopy the human condition (Baynash et al., 1994, Hosoda et al., 1994, Schuchardt et al., 1994, Durbec et al., 1996, Sanchez et al., 1996). Hirschsprung disease can present alone or as a component of Waardenburg-Shah syndrome that includes deafness and pigmentation abnormalities, reflecting the contributing role of these signaling pathways in other tissues, but colonic aganglionosis is the defining condition of this syndrome. Hirschsprung disease is also a prototypical example of a large class of congenital syndromes and adult cancers collectively called neurocristopathies that involve neural crest cells as a common etiologic factor (Mueller and Goldstein, 2022).

Placodes are bilateral condensations of the cranial surface ectoderm that generate migratory neurons and other cell types in a manner that is similar to neural crest (Baker and Bronner-Fraser, 2001). Placodes and neural crest jointly contribute to many cranial ganglia, including the Xth cranial (vagus/nodose) ganglia. While neural crest gives rise to a variety of neuronal subtypes and

glia, neurogenic placodes are only known to give rise to sensory neurons (D'Amico-Martel and Noden, 1983). The contribution of the placode cell lineage has only been recognized in the head but never before associated with the ENS.

In a recent analysis (Tan et al., 2023), we used Pax2Cre to label the placode lineage and Wnt1Cre to label the neural crest cell lineage in mice to demonstrate their contributions to specific components of the auditory system. As documented in past studies (D'Amico-Martel and Noden, 1983, Barald and Kelley, 2004, Ladher et al., 2010) and as reiterated in our study with Pax2Cre and Wnt1Cre as lineage markers (Tan et al., 2023), the placode and neural crest cell lineages have distinct and independent fates in the inner ear. Auditory functionality requires endothelin (specifically Edn3) signaling through the endothelin receptor Ednrb in both lineages, although these requirements are separable and independent and have different consequences, such that perturbation of either results in congenital deafness.

In this study, we have used Pax2Cre and Wnt1Cre to address the contribution of these cell lineages to the ENS. We demonstrate that CGRP-immunoreactive colonic myenteric mechanosensory neurons are uniquely labeled by Pax2Cre, whereas NOS^{+} inhibitory motor neurons are uniquely derived from the Wnt1Cre lineage. Importantly, Edn3-Ednrb, a signaling axis previously defined to be important for enteric neural crest cell migration, also controls the migration of Pax2Cre-labeled enteric progenitor cells, such that conditional *Ednrb* mutation driven by Pax2Cre or Wnt1Cre both result in compromised gut motility. We further show that GDNF-Ret signaling is required in both lineages to support ENS progenitor cell migration, albeit in a manner that intersects with Edn3-Ednrb signaling differently in Wnt1Cre-derived and Pax2Cre-derived cells. Our findings implicate a dual lineage origin for the ENS with mechanistically distinct features, and illuminate the consequences of Edn3 and GDNF signaling that account for Hirschsprung disease when either is compromised.

Results

Impaired colonic peristalsis in the absence of Pax2Cre-derived ENS cells in the distal colon

In our recent study addressing the placode lineage contribution to auditory development in mouse models for Waardenburg-Shah syndrome (Tan et al., 2023), we generated neural crest-specific (using Wnt1Cre) and placode-specific (using Pax2Cre) conditional *Ednrb* homozygous mutant mice (designated as *Wnt1Cre/Ednrb* and *Pax2Cre/Ednrb* respectively). In the outbred ICR background of our colony, we found that neither *Wnt1Cre/Ednrb* mutant nor *Pax2Cre/Ednrb* mutant mice lived beyond 3 weeks of age (Tan et al., 2023). The postnatal lethality of *Wnt1Cre/Ednrb* mutants around day P21 was predicted because of the well-established role of Edn3-Ednrb signaling in enteric neural crest migration and colonization (Baynash et al., 1994, Hosoda et al., 1994). However, the occurrence (and full penetrance) of lethality around this same time in *Pax2Cre/Ednrb* mutants was unexpected, as there was no prior implication that placode cells contribute to the ENS or do so in an endothelin signaling-dependent manner. *Pax2Cre/Ednrb* mutant mice exhibited growth retardation and reduced weight gain comparable to global *Ednrb* and conditional *Wnt1Cre/Ednrb* mutants in the second postnatal week (**Figure 1a**, 1b). Dissection and inspection of the gastrointestinal tract revealed that *Pax2Cre/Ednrb* mutants suffer from colonic distention and constriction similar to global *Ednrb* and *Wnt1Cre/Ednrb* mutant mice (**Figure 1d**), associated with near complete abrogation of defecation (**Figure 1c**). These observations indicate that *Ednrb*-deficiency in the Pax2Cre lineage impairs colonic peristalsis.

To visualize the contribution of Pax2Cre-derived cells to the ENS and its dependence on endothelin signaling, we crossed the $R26^{lacZ}$ reporter into the *Pax2Cre/Ednrb* background and visualized Pax2Cre-labled cells during ENS progenitor cell migration and colonization. We conducted a

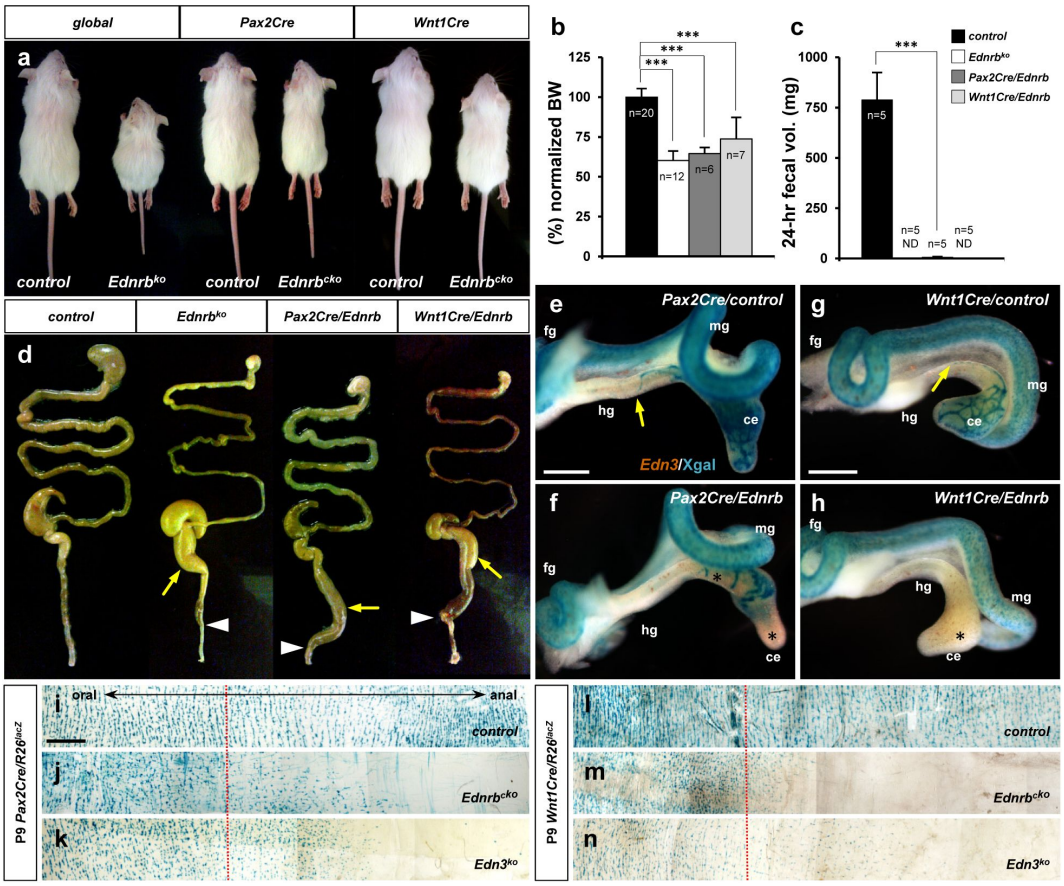

Figure 1.

Pax2Cre/Ednrb mutants mice exhibit impaired colonic peristalsis.

(a) External appearances of 3-week-old global *Ednrb* (left), *Pax2Cre/Ednrb* (middle) and *Wnt1Cre/Ednrb* (right) mutant mice compared to their littermate controls. **(b,c)** Compiled representation of normalized body weights (b) and 24-hour fecal elimination (c) from P18 mice of indicated genotypes. Error bars; mean±s.e.m. ND; not detected. P-value: ***$p<0.001$. **(d)** External appearances of P18 guts from the indicated genotypes. Arrows indicate distention of colon. Arrowheads point to constriction in the distal colon. **(e-h)** Wholemount preparations of E12.5 guts isolated from *Pax2Cre/Ednrb/R26*^{lacZ} (f), *Wnt1Cre/Ednrb/R26*^{lacZ} (h) mutant embryos and their littermate controls (e and g, respectively) stained with Xgal and labeled by *in situ* hybridization for *Edn3* expression (brown). Yellow arrows denote *Pax2Cre*-labeled (e) or *Wnt1Cre*-labeled (g) Xgal^{+} cells reaching the proximal-distal colon junction in control embryos, whereas *Ednrb*-deficient *Pax2Cre*-labeled cells (f) or *Wnt1Cre*-labeled cells (h) are deficient in caudal migration (asterisks) at the time when the *Edn3* gene is normally expressed. **(i-n)** Wholemount preparations of P9 distal colons isolated from *Pax2Cre/Ednrb* (j), *Edn3* null (k), and control (i) mice, and *Wnt1Cre/Ednrb* (m), global *Edn3* null (n), and control (l) mice stained with Xgal to visualize lineage-labeled cells. Dotted lines indicate the junction between supply by the superior mesenteric and inferior mesenteric arteries, the latter being the vascular source for the distal colon. Abbreviations: ce, cecum; fg, foregut; hg, hindgut; mg, midgut. Scale bars, 500μm (e-f, g-h), 1000μm (i-n).

parallel analysis for the Wnt1Cre lineage. Fate mapping with *Pax2Cre/R26*^{lacZ} in normal embryos showed labeled cells reaching the midgut loop at E11.5, reaching the mid-hindgut junction at E12.5, and nearly completing the colonization of the hindgut by E13.5 (Figure 1 – figure supplement 1f-h, **Figure 1e**). A comparable pattern was observed with Wnt1Cre-derived migratory cells (Figure 1 – figure supplement 1b-d, **Figure 1g**), and this temporal pattern has been previously observed using a variety of non-lineage-dependent markers of enteric progenitors (Lake and Heuckeroth, 2013). *Ednrb*-deficient Pax2Cre lineage labeled cells (**Figure 1f**) and *Ednrb*-deficient Wnt1Cre-derived cells (**Figure 1h**) both failed to advance beyond the cecum by E12.5, and this ultimately resulted in a lack of cells from both lineages in the distal colon (hindgut-derived) of postnatal mice (**Figure 1j**, 1m). *Pax2Cre/R26*^{lacZ}and *Wnt1Cre/R26*^{lacZ} mice homozygous for a global *Edn3* mutant allele also exhibited an absence of lineage-labeled cells in the distal colon (**Figure 1k**, 1n), demonstrating that migration failure is for lack of endothelin signaling and not some artifact of the conditional *Ednrb* allele. *Edn3* ligand was expressed normally in the developing gut mesenchyme of both *Ednrb* conditional mutant backgrounds (**Figure 1f**, 1h). These results indicate that the Wnt1Cre lineage and the Pax2Cre lineage both populate the hindgut, and that both lineages utilize Edn3-Ednrb signaling for migration and colonization of the hindgut.

Wnt1Cre and Pax2Cre define distinct ENS cell lineages

In the inner ear, the distinct and nonoverlapping fates of the Pax2Cre and Wnt1Cre cell lineages correspond precisely to placodal and neural crest fates as defined by prior studies (Tan et al., 2023). In addition to all known placode progeny (e.g. otic vesicle (Figure 1 – figure supplement 1i) and its later derivatives in the inner ear and cranial ganglia (Figure 1 – figure supplement 1j-l), Pax2Cre is active in several other cell types. Pax2Cre activity was detected in the ventral neural tube (Figure 1 – figure supplement 1i), which does not overlap the Wnt1Cre-active (dorsal) domain. Additional Pax2Cre active cell types include limb mesenchyme (Figure 1 – figure supplement 1e) and intermediate mesoderm and its derivatives (the mesonephric ducts and then later also in the ureteric bud) (Figure 1 – figure supplement 1e, 1o), although these sources are not migratory or neurogenic. Pax2Cre activity was not detected in several known postotic cranial/cardiac and trunk neural crest derivatives including dorsal root ganglia and sympathetic ganglia (Figure 1 – figure supplement 1m, 1n) and mesenchyme of the cardiac outflow tract (Figure 1 – figure supplement 2c). Despite this specificity, a trivial explanation for the occurrence of Hirschsprung disease phenotypes in both *Wnt1Cre/Ednrb* and *Pax2Cre/Ednrb* mutants could be if both Cre drivers recombine in the same cell populations of the ENS. As it is not possible to combine the two Cre alleles together to visualize their separate (or potentially overlapping) recombination domains, we addressed this by using molecular markers at the initial onset of their embryonic migration and in terms of the terminal (postnatal) fates of each lineage. The results, described below, confirm that Wnt1Cre and Pax2Cre define distinct ENS lineages.

First, we examined the expression domain of Pax2 protein with respect to the recombination domains of Pax2Cre and Wnt1Cre at the very early enteric progenitor migratory stage (E9.5-10.0). Prominent endogenous Pax2 was detected in the lens and otic vesicle (both known placode derivatives), in intermediate mesoderm (future kidneys), and germane to this report also in the postotic pharyngeal arches that abut vagal neural crest (Figure 1 – figure supplement 2a-b). Pax2 protein overlapped Pax2Cre-labeled pharyngeal ectoderm and Pax2Cre-labeled mesenchymal cells just at the stage of delamination from the ectoderm, although Pax2 expression was downregulated with migration and therefore not detected in most Pax2Cre lineage-labeled mesenchymal cells in the postotic domain (Figure 1 – figure supplement 2c-d). In contrast, Pax2 expression was excluded from the territory of pharyngeal neural crest marked by the Wnt1Cre lineage label (Figure 1 – figure supplement 2e-f).

We also examined expression of neural crest markers AP2 (Mitchell et al., 1991) and Sox10 (Southard-Smith et al., 1998). AP2 and Sox10 were both detected within postotic migratory pharyngeal cells (Figure 1 – figure supplement 3a-b). We observed that the entirety of Wnt1Cre-

labeled cells expressed AP2 (Figure 1 – figure supplement 3e-f). Sox10 expression was associated with a subset of the Wnt1Cre-labeled cell population, and thus with a subset of AP2-expressing arch mesenchymal cells (Figure 1 – figure supplement 3e-f). In contrast, although there was overlap of AP2 expression with Pax2Cre in the ectoderm, neither AP2 nor Sox10 were expressed in any migratory Pax2Cre lineage-labeled cells (Figure 1 – figure supplement 3g-h).

We then examined the enteric progenitor marker Ret during the early stage of enteric progenitor migration in the gut (E10.0-10.5) in normal *Pax2Cre/R26*$^{nT\text{-}nG}$ and *Wnt1Cre/R26*$^{nT\text{-}nG}$ embryos by 2-color immunohistochemistry for nuclear-GFP and Ret (**Figure 2**). We quantified the number of nGFP-positive, Ret-positive, and nGFP and Ret-double positive cells; cells that did not express either the lineage marker or Ret were excluded from measurement as these are indistinguishable from all other cell types that are present in the gut. In *Pax2Cre/R26*$^{nT\text{-}nG}$ embryos (6 embryos from different litters, average 249.7±5.7 counted cells per embryo), only 11.8±1.6% of the counted cells were Pax2Cre-derived (**Fig. 2v**, black and grey bars); the other 88% (**Fig. 2v**, white bar) are presumed to be Wnt1Cre-derived Ret^{+} cells (which was directly measured at 86% as described below). Ret was expressed in 14.4±1.7% of the Pax2Cre lineage-labeled cells, but only 1.6±0.2% of the total counted cells. We performed the same analysis for the Wnt1Cre lineage (6 embryos; 178.8±11.4 counted cells per embryo). Here, almost all (97.8±0.2%) counted cells were lineage labeled, and of these, 86.2±1.5% expressed Ret. Only 2.2±0.2% of counted cells in *Wnt1Cre/R26*$^{nT\text{-}nG}$ embryos expressed Ret but were lineage-negative; these are presumably Pax2Cre-derived, which was directly measured at 1.6% as described above. Consequently, 97.5% of the Ret-expressing cells in *Wnt1Cre/R26*$^{nT\text{-}nG}$ embryos were of this lineage. Approx. 10-15% of lineage labeled cells in both analyses did not express Ret (**Figure 2v** grey bars). These results indicate that Ret-expressing cells in the E10.5 midgut are overwhelmingly derived from the Wnt1Cre lineage. The majority of Wnt1Cre-derived cells at E10.5 in the midgut express Ret whereas only a minor population of Pax2Cre-derived cells does so. This further supports the idea that Pax2Cre and Wnt1Cre delineate molecularly distinct populations of early migratory ENS progenitor cells.

We next evaluated expression of markers in normal P9 pups that were also lineage labeled with Pax2Cre or Wnt1Cre crossed with *R26* reporters. First, based on morphology and expression of the pan-neuronal marker Hu, approximately half of colonic myenteric ganglion cells were labeled with either lineage marker (Figure 3 – figure supplement 1a-b, 1g pie chart). Because the sum of the two individual estimates is close to 100%, this is consistent with the proposition that all or most ENS neurons are derived from either a Pax2Cre or a Wnt1Cre lineage and that the two Cre lines are mostly if not fully nonoverlapping in their recombination domains. That is, if there was an appreciable degree of overlap between the two lineages, an equal fraction of Hu^{+} neurons would have to be derived from a third source, for which there is no evidence.

As summarized earlier, colonic peristalsis is facilitated by an integrated circuitry from mechanosensory neuron to interneuron to motor neuron to muscle contraction (**Figure 3a**). Electrophysiology studies of guinea pig colon showed that mechanosensory neurons release the excitatory neurotransmitter calcitonin gene related peptide (CGRP) to initiate peristaltic contractions (Sarna, 2010). By immunostaining, we identified that CGRP^{+} neurons in the postnatal P9 mouse distal colon are located in the myenteric plexus and send their projections to the gut luminal epithelium, consistent with a mechanosensory fate (**Figure 3b**). Nitric oxide synthase (NOS) is recognized as a marker for both inhibitory interneurons and inhibitory motor neurons (Costa et al., 1992, Timmermans et al., 1994, Sang and Young, 1996). In the mouse P9 colon, NOS^{+} neurons are found in the myenteric ganglia and their axons are found exclusively within the circular muscle layer (**Figure 3c**), implying that these represent at least a subset of motor neurons. Interneurons are not readily identifiable with this circular cross section analysis because of their exclusively interganglionic (mostly ascending/descending) projections.

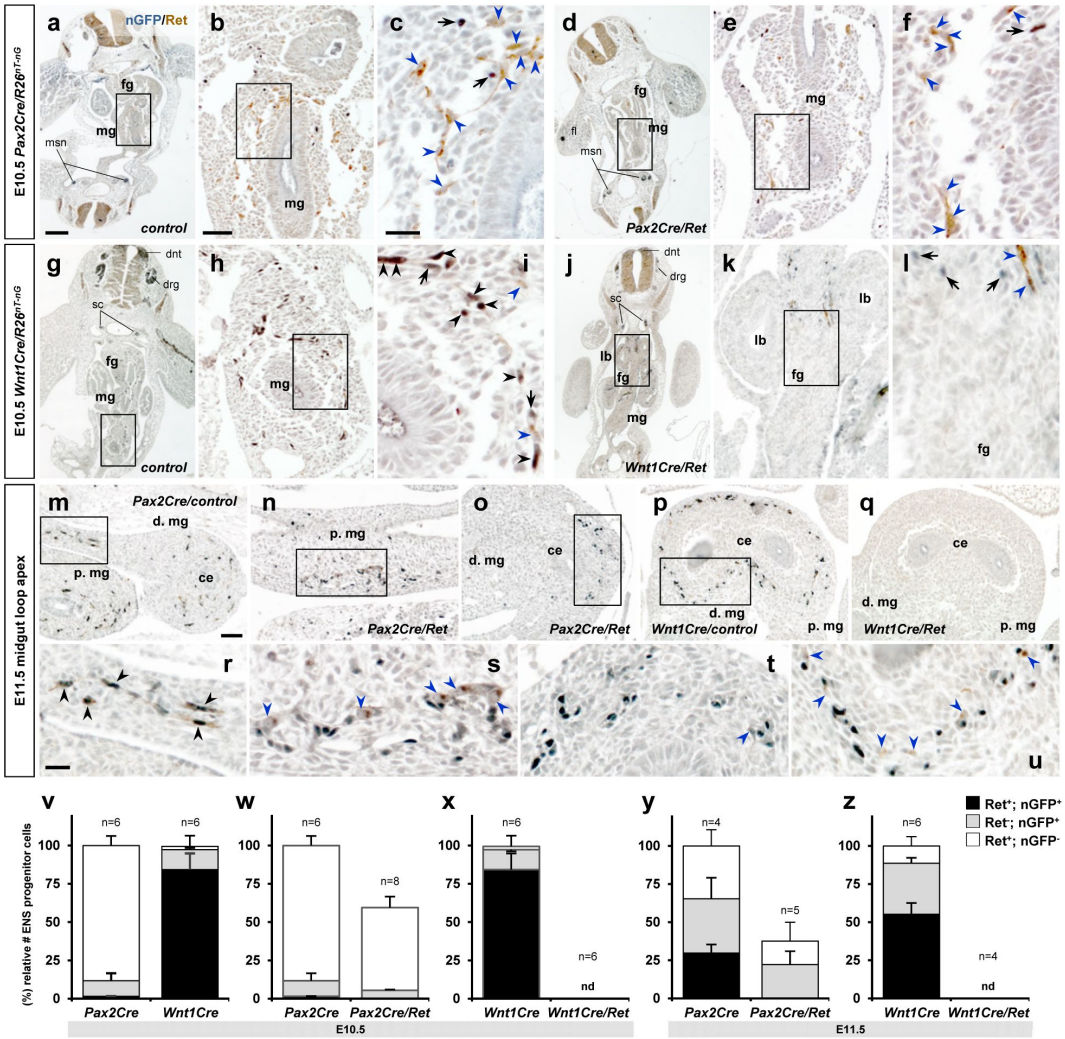

Figure 2.

Developmental transition of Ret expression in migratory ENS progenitor cells.

(a-u) Histological sections prepared from E10.5 *Pax2Cre/Ret/R26*$^{nT\text{-}nG}$mutant (d-f), *Wnt1Cre/Ret/R26*$^{nT\text{-}nG}$ mutant (j-l), and their littermate controls (a-c, and g-I, respectively), and E11.5 *Pax2Cre/Ret/R26*$^{nT\text{-}nG}$ mutant (n-o), *Wnt1Cre/Ret/R26*$^{nT\text{-}nG}$ mutant (q), and their littermate control embryos (m and p, respectively) stained for nuclear-GFP (blue) and Ret (brown). Magnified views of the bracketed areas (midgut) in a, d, g and j are shown in b, e, h and k, respectively; of the bracketed areas in b, e, h and k are shown in c, f, I and l, respectively; of the bracketed areas in m-p are shown in r-u, respectively. Black arrows denotes lineage marker nGFP^{+} nuclei with no Ret stain, black arrowheads denoted cells that are positive for both nuclear GFP and Ret, and blue arrowheads denote non-Cre (nGFP^{-}) Ret^{+} cells along the gut walls. **(v-z)** Compiled representations of relative fractions of Ret^{+},nGFP^{+} (black); Ret^{-},nGFP^{+} (grey); and Ret^{+},nGFP^{-} (white) ENS progenitor cells comparing (v) E10.5 midgut areas of *Pax2Cre/R26*$^{nT\text{-}nG}$ (n=6; 249.7±15.7cells/embryo) and *Wnt1Cre/R26*$^{nT\text{-}nG}$ (n=6; 178.83±11.41 cells/embryo) embryos, (w) E10.5 midgut areas of *Pax2Cre/Ret/R26*$^{nT\text{-}nG}$ mutants (n=8, 148.50±12.13 cells/embryo) and littermate control embryos, (x) E10.5 midgut areas of *Wnt1Cre/Ret/R26*$^{nT\text{-}nG}$ mutants (n=6, no nGFP^{+} or Ret^{+} cell was found) and littermate control embryos, (y) E11.5 midgut loop apex areas of *Pax2Cre/Ret/R26*$^{nT\text{-}nG}$mutants (n=5, 309.33±18.57 cells/embryo) and littermate control embryos (n=4, 822.67±28.30 cells/embryo), and (z) E11.5 midgut loop apex areas of *WntCre/Ret/R26*$^{nT\text{-}nG}$ mutants (n=4, no nGFP^{+} or Ret^{+} cell was found) and littermate control embryos (n=6, 986.40±89.24 cells/embryo). Data in v are the control mouse groups in w and x, shown together for easier comparison. Ret^{-},nGFP^{-} (double negative) cell populations were not included in this analysis. nd=not detected. Abbreviations: dnt, dorsal neural tube; drg, dorsal root ganglia; msn, mesonephros; sc, sympathetic chain ganglia. Scale bars, 200μm (a, d, g, j), 50μm (b, e, h, k, m-q), 20μm (c, f, i, l, r-u).

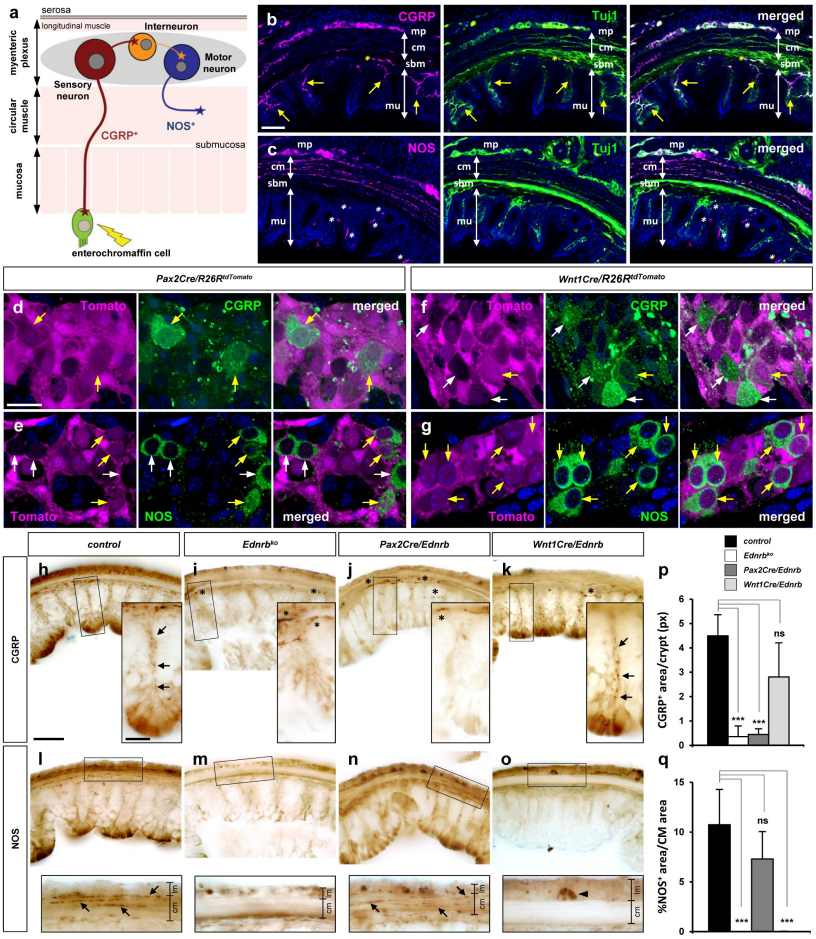

Figure 3.

Mechanosensory fate of *Pax2Cre* lineage and selective loss of CGRP$^+$ myenteric mechanosensory axons in *Pax2Cre/Ednrb* mutant distal colon.

(a) Schematic illustration of neuronal subtypes in the colonic myenteric ganglia and their endorgans. Mechanosensory neurons (red) extend their peripheral axons to the mechanosensory (enterochromaffin) cells while their other axons synapse to interneurons (orange). Motor neurons (blue) innervate the colonic circular muscle to generate colonic peristalsis. **(b-c)** Confocal images of transverse sections of the distal colon co-immunostained for CGRP and Tuj1 (b) or NOS and Tuj1 (c) show selective label of sensory and motor axons by CGRP (b) and NOS (c), respectively. Yellow arrows in b denote CGRP$^+$ axons that project through each crypt to reach enteric epithelium. Yellow asterisks in b indicate CGRP$^+$ axons from pelvic ganglia along the submucosal layer. White asterisks in c point to NOS-reactive non-neuronal epithelial cells of the mucosa. **(d-g)** Confocal images of the myenteric ganglia of P9 distal colons isolated from *Pax2Cre/R26^{tdTomato}*(d-e) and *Wnt1Cre/R26^{tdTomato}* (f-g) mice immunostained for CGRP (d, f) and NOS (e, g). Low magnification views from which these images were taken are shown in Supplemental Figure S4. Compared to b and c, this wholemount preparation emphasizes cell bodies in the myenteric plexus rather than axon projections. Yellow arrows point to lineage marker-positive CGRP$^+$ or NOS$^+$ neurons, whereas white arrows indicate lineage marker-negative CGRP$^+$ or NOS$^+$ neurons of the myenteric ganglia. **(h-o)** Serial transverse vibratome sections of the transition areas (see Supplemental Figure S6c, 6h) of the distal colons isolated from P9 control (h, l), global *Ednrb* (i, m), *Pax2Cre/Ednrb* (j, n) and *Wnt1Cre/Ednrb* (k, o) mutants immunostained for CGRP (h-k) or NOS (l-o). Magnified views of bracketed areas are shown in the insets. Arrows in h and k denote CGRP$^+$ axonal projections toward mucosal epithelium in a single crypt. Arrows in l and n denote NOS$^+$ axonal projections perforating throughout the circular muscle layer. Arrowhead in o indicates a NOS$^+$ presumed myenteric interneuron (because it lacks motor axons in the circular muscle layer) of *Wnt1Cre/Ednrb* mutant colon. **(p)** Complied representation of the average pixel values of CGRP$^+$ axon area per single crypt. **(q)** Complied representation of the average fraction of NOS$^+$ axon area in the circular muscle area. Analysis includes 24 crypts from 8 distal colon sections per genotype (four controls, two *Ednrb*, three *Pax2Cre/Ednrb* and three *Wnt1Cre/Ednrb* mutants). P-values: ***$p<0.001$, ns=not significant. Error bars, mean±s.e.m. Scale bars, 50μm (b-c, h-o), 20μm (d-g, h-o insets). Abbreviations: cm, circular muscle; lm, longitudinal muscle; mp, myenteric plexus; mu, mucosa; sbm, submucosa.

To discern the lineage origins of these mature cell types, we evaluated the expression of these markers in lineage-labeled P9 pups. Only approximately one-third of neurons of both lineages in the distal colon were CGRP$^+$ or NOS$^+$ (Figure 3 – figure supplement 1g bar graph), which means that additional neuronal fates (white bars in Figure 3 – figure supplement 1g) are taken by both lineages (which is expected). Less than 10% of myenteric ganglion neurons were CGRP$^+$ (Figure 3 – figure supplement 1h pie chart). Strikingly, the vast majority (>90%) of these were Pax2Cre-derived (**Figure 3d**, Figure 3 – figure supplement 1c-d, 1h bar graph). A minimum number (approx. 3%) of CGRP$^+$ neurons were labeled by Wnt1Cre (**Figure 3f**, Figure 3 – figure supplement 1, 1h bar graph), which indicates that Wnt1Cre-derived cells have little or no commitment to a mechanosensory fate in the distal colon. Approx. 25% of myenteric ganglion neurons were NOS$^+$. The majority of these were derived from the Wnt1Cre lineage (**Figure 3g**, Figure 3 – figure supplement 1f, 1h bar graph), although Pax2Cre-derived neurons also gave rise to a NOS-reactive population of the distal colon (**Figure 3e**, Figure 3 – figure supplement 1e, 1h bar graph). As mentioned above, NOS identifies both inhibitory interneurons and inhibitory motor neurons in the intestine, so these results do not by themselves indicate if Pax2Cre-labeled NOS$^+$ and Wnt1Cre-labeled NOS$^+$ neurons are the same or different fates (this point is addressed below in lineage-specific *Ednrb* mutants).

If Pax2Cre and Wnt1Cre label distinct subsets of ENS neurons in normal mice, a prediction is that these subsets might be selectively ablated in lineage-specific *Ednrb* mutant mice. To address this, we immunohistochemically analyzed axonal projections from the myenteric plexus in serial sections of the colons of both lines of mutant mice at P9. Importantly, sections were taken at the transition between ganglionic and aganglionic areas (Figure 3 – figure supplement 3c-d, 3g-h). Adjacent sections were stained for CGRP or NOS. In this transition zone, we observed a profound reduction of CGRP$^+$ axons projecting towards the colonic lumen in *Pax2Cre/Ednrb* mutant guts (**Figure 3j**, 3p), equal to that in global *Ednrb* mutants (**Figure 3i**, 3p), whereas NOS$^+$ axons in the circular muscle were present normally in the adjacent section (**Figure 3n**, 3q). There were some CGRP$^+$ axons projecting longitudinally along the submucosal layer (**Figure 3j** asterisks), although these most likely originate from sacral neural crest-derived pelvic ganglion neurons (Figure 3 – figure supplement 2) or trunk neural crest-derived DRG neurons (Wolfson et al., 2023), and were also detected in the global *Ednrb* mutant gut (**Figure 3i** asterisks).

Wnt1Cre/Ednrb mutant guts exhibited abundant CGRP$^+$ axons projecting toward sensory epithelium (**Figure 3k**, 3p) while their circular muscle layers showed a total loss of NOS$^+$ axonal innervation (**Figure 3o**, 3q). NOS$^+$ neurons were still present in the myenteric plexus of the *Wnt1Cre/Ednrb* mutant distal colon (**Figure 3o** inset arrowhead); as these neurons project neither to sensory nor motor targets, we suspect that these are interneurons and likely originate from the Pax2Cre lineage. Thus, in the transition area, defective migration of Pax2Cre-derived enteric progenitor cells results in selective loss of myenteric mechanosensory neurons, while myenteric motor neurons and their innervations of the circular muscle were not affected. Reciprocally, defective migration of Wnt1Cre-derived ENS progenitors results in selective loss of motor neurons with no impact on the mechanosensory neuron population.

These results collectively demonstrate that Pax2Cre-labeled and Wnt1Cre-labeled cells have a distinct and nonoverlapping marker expression program during their embryonic migration, and have a distinct set of terminal differentiation fates in the postnatal distal colon. A further conclusion from the analysis of conditional *Ednrb* mutants is that neither lineage can modulate its normal fate to compensate for the absence of the other.

Pax2Cre lineage-specific *Ret* mutant embryos exhibit defective enteric progenitor migration

ENS development requires a functional GDNF-Ret signaling axis alongside that of Edn3-Ednrb. The unexpected observation that Ednrb function is required in both the Wnt1Cre and Pax2Cre domains in ENS development led us to also address Ret function in these lineages. A previous study (Luo et al., 2007) documented Hirschsprung disease phenotypes in mice with conditional Ret mutation in the Wnt1Cre domain (*Wnt1Cre/Ret* mutants), including lethality around postnatal day 21. Global *Ret* deficiency results in neonatal lethality because of renal agenesis (Schuchardt et al., 1994, Durbec et al., 1996), and because Pax2Cre is expressed in intermediate mesoderm, *Pax2Cre/Ret* mutants in our colony also died in the early postnatal period. We therefore explored the consequences of *Ret* deficiency in the Pax2Cre lineage during embryonic enteric progenitor cell migration. In *Pax2Cre/Ret/R26*^{lacZ} mutant embryos at E12.5, we observed an obvious deficiency of Pax2Cre-labeled cells migrating throughout the midgut, and no Pax2Cre-labeled cells migrated caudally beyond the cecum (**Figure 4b**), whereas lineage-labeled cells reached the terminal hindgut in littermate controls (**Figure 4a**). This result implies a function for Ret within the Pax2Cre lineage. This was surprising because the expression analysis in normal embryos described above indicated that so few (1.6%) of the ENS progenitors at E10.5 are of the Pax2Cre lineage and are Ret^{+} (**Figure 2a-c**, 2v).

We considered whether Ret expression in the Pax2Cre lineage changes around E10.5 that might account for these observations. We found that a substantially larger fraction of Pax2Cre-labeled cells in the distal midgut (at the migratory wavefront) in control E11.5 *Pax2Cre/R26*$^{nT\text{-}nG}$ embryos expressed Ret (**Figure 2m**, 2y black bar) relative to E10.5 (**Figure 2w**, black bar). This demonstrates that the Pax2Cre-labeled population in control embryos expands significantly during the E10.5-11.5 period. This could occur by proliferation of the very small Ret^{+} population that was present at E10.5, or could occur by conversion of Ret^{-} to Ret^{+} cells within the lineage, or both, and perhaps was already just underway at E10.5. Obviously, at both E10.5 and E11.5, there were no Ret^{+} cells in the Pax2Cre lineage in *Pax2Cre/Ret* mutants (**Figure 2n-o**, 2w, 2y).

We next performed wholemount staining with the neural progenitor marker p75 (at E10.5) or with the pan-neuronal marker 2H3 (at E12.5) on guts isolated from *Pax2Cre/Ret/R26*$^{td\text{-}Tomato}$mutants and their littermate controls. This allowed us to visualize the Pax2Cre lineage in *Pax2Cre/Ret* mutant embryos alongside other neuronal lineages (i.e., the Wnt1Cre lineage) in which Ret function is intact. At E10.5, p75-expressing enteric progenitors included Pax2Cre lineage cells co-migrating with non-Pax2Cre cells (**Figure 4i**), the latter which presumably consists of Wnt1Cre-derived cells. In *Pax2Cre/Ret* mutant embryos at this stage, p75-expressing cells again included those with and without the Pax2Cre lineage label, demonstrating a normal caudal progression (**Figure 4j**). Histological Ret expression analysis in *Pax2Cre/Ret/R26*$^{nT\text{-}nG}$embryos clearly showed that some migratory progenitor cells express Ret (**Figure 2d-f**). Since *Ret* is knocked out in *Pax2Cre/Ret* mutants, these Ret^{+} cells are presumed to be Wnt1Cre-derived. Quantitative evaluation, however, indicated that overall ENS progenitor cell number was already affected as early as E10.5 in the *Pax2Cre/Ret* mutant background (**Figure 2w**): both the Pax2Cre-derived cell population and the Ret-expressing non-Pax2Cre population were reduced by half, and therefore the total number of countable cells (expressing one or both markers) per midgut from each mutant embryo was also reduced by half. A somewhat larger reduction in total countable cells was observed in *Pax2Cre/Ret* mutants at E11.5 (**Figure 2y**) compared to E10.5 (**Figure 2w**). Consequently, at E12.5, compared to control littermate (**Figure 4e**), *Pax2Cre/Ret* mutants showed a marked deficiency of 2H3-positive cells though the midgut loop, and no 2H3 signal was detected caudal to the cecum (**Figure 4f**). The interpretation of this analysis is that *Ret* deficiency in the Pax2Cre lineage impacts ENS progenitor cells derived from the Pax2Cre lineage as well as from the presumptive Wnt1Cre lineage, starting as the migratory cells enter the midgut.

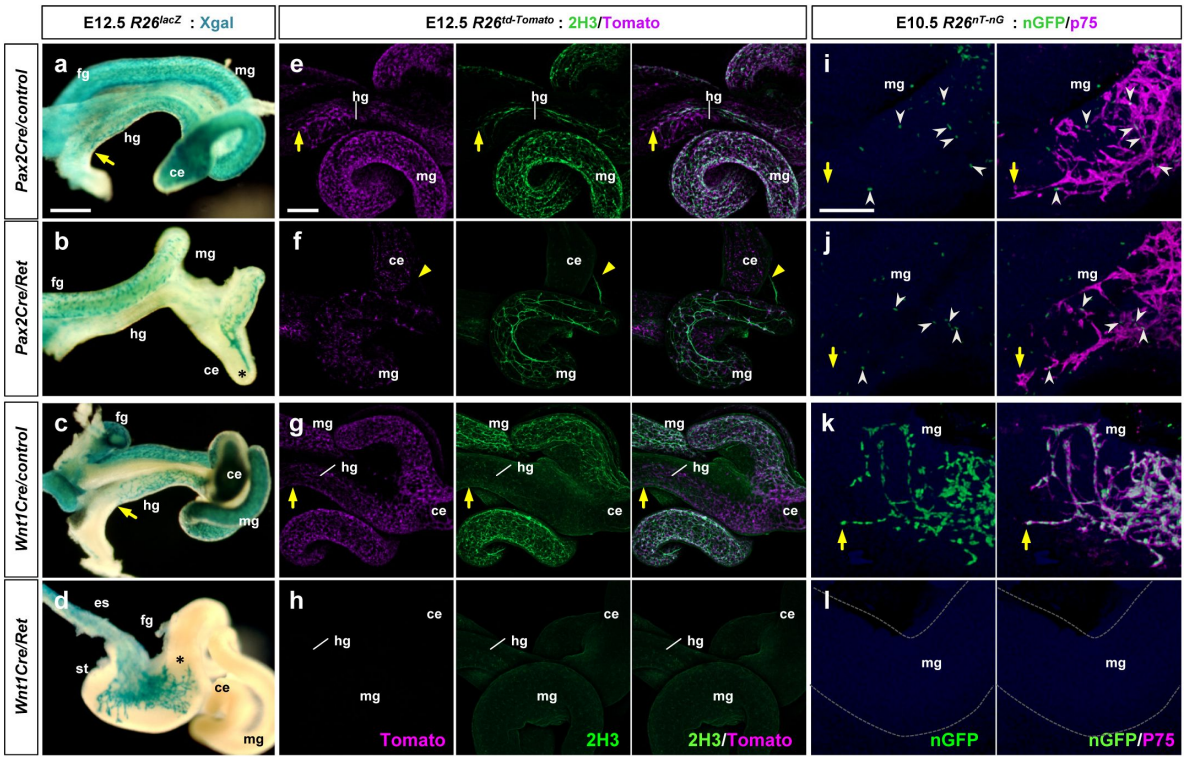

Figure 4.

Pax2Cre-specific deletion of *Ret* results in defective ENS progenitor migration and differentiation.

(a-d) Wholemount preparations of E12.5 guts isolated from *Pax2Cre/Ret/R26*^{lacZ}(b), *Wnt1Cre/Ret/R26*^{lacZ} (d) mutant embryos and their littermate controls (a and c, respectively) stained with Xgal (blue). Arrows denote the wavefronts of lineage-labeled cells in the hindguts of the controls. Asterisks denote halted migration of *Ret*-deficient *Pax2Cre*-labeled cells at the cecum (b) and of *Ret*-deficient *Wnt1Cre*-labeled cells at the caudal end of the stomach (d). **(e-h)** Wholemount preparations of E12.5 guts isolated from *Pax2Cre/Ret/R26*$^{td\text{-}Tomato}$(f), *Wnt1Cre/Ret/R26*$^{td\text{-}Tomato}$ (h) mutant embryos and their littermate controls (e and g, respectively) stained for neuronal 2H3 (green). Arrows denote the wavefronts of lineage-labeled cells in the hindguts of the control embryos. Arrowheads denote halted migration of *Ret*-deficient *Pax2Cre*-labeled cells at the cecum (f). **(i-l)** Wholemount preparations of E10.5 guts isolated from *Pax2Cre/Ret/R26*$^{nT\text{-}nG}$(j), *Wnt1Cre/Ret/R26*$^{nT\text{-}nG}$ (l) mutant embryos and their littermate controls (i and k, respectively) stained for nuclear-GFP (green) and ENS progenitor marker p75 (magenta). Arrows denote the wavefronts of lineage-labeled cells in the midguts. Arrowheads denote p75^{+} *Pax2Cre*-labeled cells at the midgut areas (i-j). Abbreviations: es, esophagus; st, stomach. Scale bars, 500μm (a-d), 250μm (e-h), 50μm (i-l).

In parallel we also crossed the conditional *Ret* allele into the *Wnt1Cre/R26* background. Wnt1Cre-labeled cells at E12.5 populated the esophagus and stomach but failed to migrate into the intestine (**Figure 4d**), which recapitulates the global *Ret* mutant phenotype (Schuchardt et al., 1994, Durbec et al., 1996). Wholemount 2H3 staining confirmed the total loss of enteric progenitor cells along the entire axis of the developing intestine (**Figure 4h**). Defective progenitor entry into the intestinal tract was evident as early as E10.5 based on wholemount p75 staining (**Figure 4i**) as well as Ret expression analysis on histological sections prepared from *Wnt1Cre/Ret/R26*$^{nT\text{-}nG}$embryos at E10.5 (**Figure 2j-l**, 2x) and E11.5 (**Figure 2q**, 2z). It should be noted that our analysis at E10.5-12.5 precedes the E14.5 arrival of neurogenic Schwann cell precursors, which are neural crest-derived but which do not require Ret for their migration (Uesaka et al., 2015). These results demonstrate that Ret function in the Wnt1Cre domain is absolutely required for migration of all enteric progenitors, Wnt1Cre-derived as well as non-Wnt1Cre-derived (i.e., Pax2Cre-derived), into and through the intestinal tract.

To better understand how GDNF-Ret signaling influences the Pax2Cre and Wnt1Cre lineage cells, we employed collagen gel explant cultures of serial 200μm slices prepared from E10.5 midgut segments collected in a rostrocaudal sequence (Figure 5 – figure supplement 1a). After 3 days in culture we visualized td-Tomato as a lineage marker, stained for Hu as a neuronal marker, and BLBP as a glial marker. No outgrowth was observed in the absence of added factors (**Figure 5a**). Hu and BLBP were both detected within the untreated explanted gut slices (**Figure 5a**), showing that enteric progenitor cells present in the gut slices survived for three days in vitro and sustained a normal differentiation program without growth factors. GDNF induced robust radial outgrowth from control midgut slices, which included a mixed population of neurons and glia; Pax2Cre lineage cells were present in these outgrowths (**Figure 5b**). Control explants showed a progressively diminishing response along the rostrocaudal axis (**Figure 5g**), which reflects the number of enteric progenitor cells present in each slice.

Pax2Cre/Ret mutant gut explants, however, exhibited little or no outgrowth in response to GDNF (**Figure 5c**, 5g), even though lineage-positive, Hu-positive, and BLBP-positive cells are present in the explant itself. Importantly, Ret-expressing non-Pax2Cre lineage (i.e., likely Wnt1Cre-derived) cells are present throughout the midgut at E10.5 (**Figure 2f**, 2w), yet there were no lineage negative outgrowths in response to GDNF in *Pax2Cre/Ret* explants (**Figure 5c**). This indicates that the Wnt1Cre-derived cells in the midgut do not harbor a cell-autonomous migratory response to GDNF, but instead require co-migration with Pax2Cre lineage cells.

Control E10.5 *Wnt1Cre/R26*$^{td\text{-}Tomato}$midgut explants demonstrated response to GDNF at each axial level (Figure 5d-e, h), similar to *Pax2Cre/R26*$^{td\text{-}Tomato}$ explants. *Wnt1Cre/Ret* mutant gut explants showed no lineage marker, neuronal Hu, or glial BLBP positive cells along the entirety of the midgut segments, within or outgrown from the explant (**Figure 5f**, 5h), confirming the total absence of all enteric progenitor cells, including Pax2 lineage cells, in this mutant background (**Figure 4d**). Collectively, we interpret these results to show that ENS progenitor migration is an orchestrated process that requires GDNF response in both Pax2Cre and Wnt1Cre progenitor populations. To support migration, each progenitor lineage requires migratory function (i.e., Ret function) in the other, albeit at different times and locations along the gut axis: Ret deficiency in the Wnt1Cre lineage blocks migration of both lineages at the duodenum, whereas Ret deficiency in the Pax2Cre lineage blocks migration of both lineages at the hindgut.

Divergent lineage-specific regulation of Ret signaling by Edn3-Ednrb

Edn3-Ednrb and GDNF-Ret signaling are both required for caudal migration of Wnt1Cre-derived and Pax2Cre-derived enteric progenitors in vivo. We used the gut slice explant assay to address the relationship between these signaling mechanisms. Midgut slices from *Pax2Cre/R26*$^{td\text{-}Tomato}$ and *Wnt1Cre/R26*$^{td\text{-}Tomato}$ embryos were cultured in collagen beds supplemented with EDN3 or with

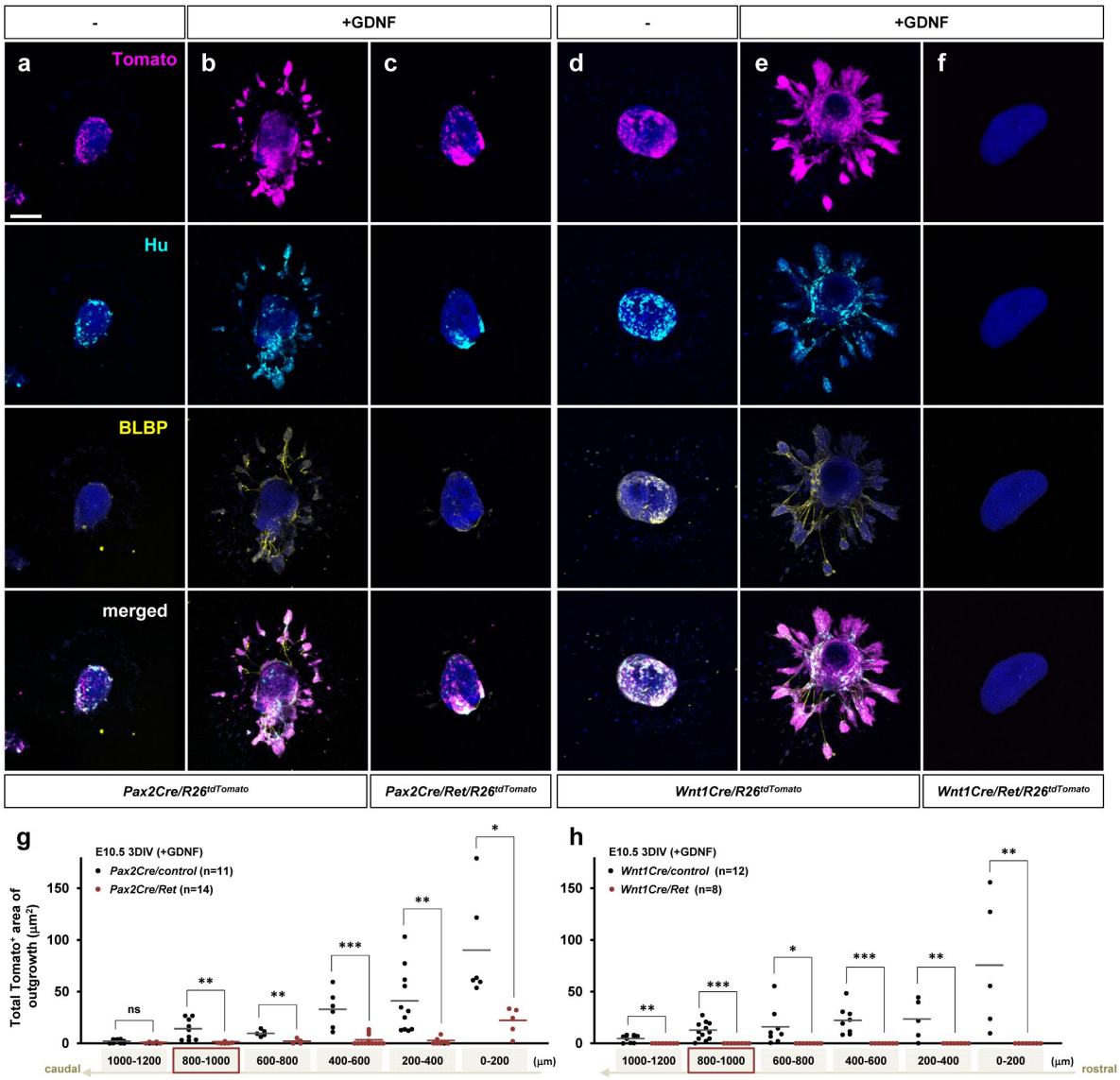

Figure 5.

Defective GDNF-induced outgrowth and differentiation of *Pax2Cre/Ret* mutant ENS progenitors in vitro.

(a-f) Confocal images of 200µm midgut sections isolated from an E10.5 *Pax2Cre/Ret/R26*$^{td\text{-}Tomato}$mutant (c) and its littermate control (a-b), and a *Wnt1Cre/Ret/R26*^{tdTomato} mutant (f) and its littermate control (d-e) cultured 3 days in vitro (3DIV) in the absence (a, d) or presence of GDNF (b-c, e-f), then immunolabeled for neuronal Hu (cyan) and glial BLBP (yellow). Scale bars, 250µm. **(g)** Complied representation of the total area of outgrowth (Tomato^{+} area around the explanted gut tube) from *Pax2Cre/control* (black dots; n=11) and *Pax2Cre/Ret* mutant (red dots; n=14) embryos in the presence of GDNF. **(h)** Compiled representation of the total outgrowth area from *Wnt1Cre/control* (black dots; n=12) and *Wnt1Cre/Ret* mutant (red dots; n=8) embryos in the presence of GDNF. See **Figure 5** – figure supplement 1a for rostrocaudal orientation of the midgut slice preparations. Each dot represents the outgrowth of each gut slice prepared from each embryos used for data acquisition (lost individual midgut sections are not included as data points). The images shown in a-f represent sections that are 800-1000 µm caudal to the foregut-midgut junction (as indicated by the red boxes in g-h). P-values: *$p<0.05$, **$p<0.01$, ***$p<0.001$, ns=not significant.

the p75 ligand NGF for 3 days in vitro. While explanted gut sections at E10.5 contain cells that express p75 and Hu, neither EDN3 nor NGF promoted enteric progenitor cell outgrowth compared to the activity of GDNF (Figure 5 – figure supplement 2). Similarly, at E11.5, EDN3 and NGF induced only minimal outgrowth from both Pax2Cre– and Wnt1Cre-lineage labeled midgut sections (Figure 6 – figure supplement 1). Impaired cell migration in vivo (**Figure 1f**, 1h) has at various times been previously interpreted in global *Edn3* and *Ednrb* mutants to represent a chemoattractive role for Edn3-Ednrb signaling, but as previously shown in vitro (Barlow et al., 2003, Goto et al., 2013, Nagy and Goldstein, 2017) and in our results, Edn3-Ednrb signaling does not by itself induce migration of either Pax2Cre-labeled or Wnt1Cre-labeled enteric progenitors.

The in vitro explant assays clearly demonstrate that GDNF-Ret signaling is the major mechanism that supports ENS progenitor migration. To address why enteric progenitor migration in vivo is defective in *Ednrb*-deficient backgrounds, we performed gut slice explant assays using E11.5 midguts isolated from *Pax2Cre/Ednrb/R26*$^{td\text{- }Tomato}$ and *Wnt1Cre/Ednrb/R26*$^{td\text{-}Tomato}$mutant embryos. Across the rostral-caudal axis of the midgut, *Pax2Cre/Ednrb* mutant explants showed a blunted response to GDNF compared to control cells (**Figure 6a**, 6c), which was more severe at the distal end (**Figure 6b**, 6d, 6i-j), even though lineage-positive cells were present. *Wnt1Cre/Ednrb* mutant midgut segments exhibited a similar trend as *Pax2Cre/Ednrb* mutant midgut in both proximal (**Figure 6e**, 6g, 6k) and distal segments (**Figure 6f**, 6h, 6l), including greater impairment of GDNF responsiveness at the migratory wavefront. These results show that the Pax2Cre and Wnt1Cre lineages both rely on endothelin signaling to fully populate the gut with GDNF-responsive cells, and imply that endothelin signaling is needed to support GDNF responsiveness in enteric progenitors.

Next we asked whether *Ednrb*-deficiency alters Ret expression in the enteric progenitor cell population. We used 2-color IHC for nuclear-GFP and Ret on histological sections prepared from E11.5 *Pax2Cre/Ednrb/R26*$^{nT\text{-}nG}$ mutant embryos and their littermate controls. As also noted earlier (**Figure 2m**, 2y), in normal E11.5 embryos a large fraction of Pax2Cre-derived cells express Ret at the migratory wavefront (**Figure 7a**, 7e). In the *Pax2Cre/Ednrb* mutant, however, Pax2Cre-labeled cells populating the apex of the midgut loop were Ret-negative, and the surrounding Ret-expressing cells were mostly unlabeled by the Pax2Cre lineage marker (**Figure 7b**, 7f). We measured the number of nGFP-positive only, Ret-positive only, and nGFP and Ret double positive cells at three different axial levels: distal midgut, caudal half of the proximal midgut (towards the cecum; equivalent to 0-600 microns in **Figure 6i**) and rostral half of the proximal midgut (towards the foregut-midgut junction; equivalent to 600-1200 microns in **Figure 6i**). The analysis confirmed that absence of *Ednrb* resulted in far fewer Pax2Cre lineage-derived cells expressing Ret in the more caudal segments (**Figure 7i**). Thus, the expansion of the Ret^{+} subpopulation of the Pax2Cre lineage that occurs between E10.5-11.5 (**Figure 2m**, 2y) requires Ednrb signaling in a cell autonomous manner. As noted earlier, this could occur via proliferation of the very small Ret^{+} population at E10.5, by induction of Ret expression in previously Ret-negative cells, or both. The important conclusion is that this process by Pax2Cre-derived cells is dependent on Ednrb.

We performed the same analysis for E11.5 *Wnt1Cre/Ednrb/R26*$^{nT\text{-}nG}$mutants and their littermate embryos (**Figure 7c-d**, 7g-h, 7j). Unlike the observation in the Pax2Cre lineage, Edn3-Ednrb signaling does not affect Ret expression in Wnt1Cre-derived migratory enteric progenitor cells. Nonetheless, these cells are unable to respond to GDNF in vivo (**Figure 1h**) and in vitro (**Figure 6g-h**).

In general, extracellular ligands of receptor tyrosine kinases (RTKs) trigger autophosphorylation of intracellular tyrosine residues that ultimately recruit intracellular adaptor proteins to initiate downstream signaling. In a variety of ways, RTK signaling can require mediation by G protein coupled receptors, a mechanisms called transactivation (Kilpatrick and Hill, 2021). Prior in vitro explant studies have implicated a convergence of Ret and Ednrb at the level of protein kinase A activity (Barlow et al., 2003, Goto et al., 2013), although other mechanisms of transactivation

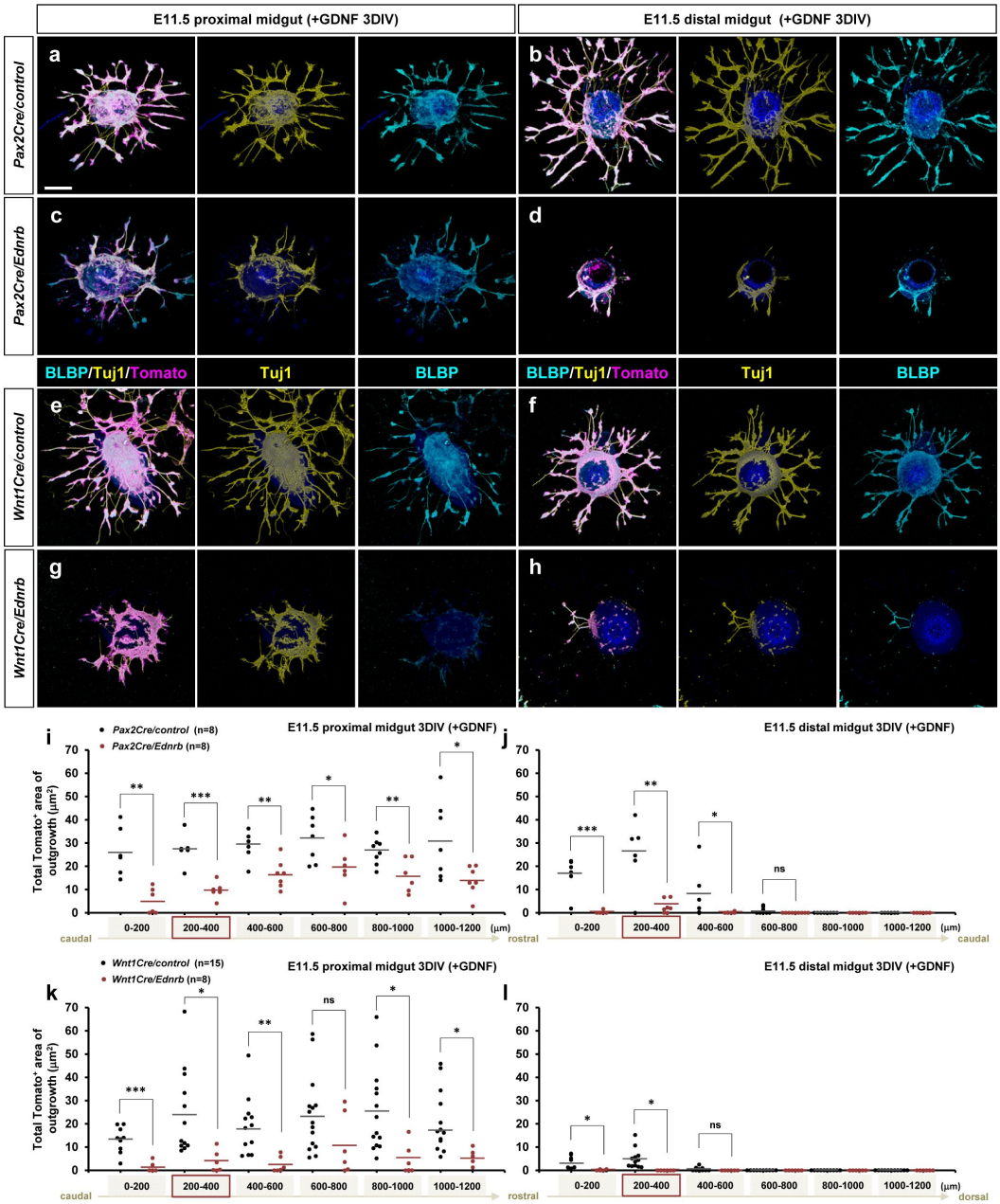

Figure 6.

Ednrb-deficient ENS progenitor cells populating the migratory wavefront exhibit attenuated response to GDNF in vitro.

(a-h) Confocal z-stack images of 200µm proximal (a, c, e, g) and distal midgut (b, d, f, h) sections isolated from an E11.5 *Pax2Cre/Ret/R26*$^{td\text{-}Tomato}$mutant (c-d) and its littermate control (a-b), and a *Wnt1Cre/Ret/R26*^{tdTomato}mutant (g-h) and its littermate control (e-f) cultured 3 days in vitro (3DIV) in the presence of GDNF and then immunolabeled for neuronal Tuj1 (yellow) and glial BLBP (cyan). Scale bars, 250µm. **(i-j)** Compiled representation of the total area of outgrowth (Tomato^{+} area around the explanted gut tube) from proximal and distal midguts of *Pax2Cre/control* (black dots; n=8) and *Pax2Cre/Ret* mutant (red dots; n=8) embryos in the presence of GDNF. **(k-l)** Compiled representation of the total area of outgrowth from *Wnt1Cre/control* (black dots; n=15) and *Wnt1Cre/Ret* mutant (red dots; n=8) embryos in the presence of GDNF. See **Figure 5** – figure supplement 1b for rostrocaudal orientation of the midgut slices. The proximal midgut images shown in a,c,e,g represent sections that are 200-400 µm rostral to the apex of the midgut loop; the distal midgut images shown in b,d,f,h represent sections that are 200-400 µm caudal to the apex of the midgut loop (as indicated by the red boxes in i-l). P-values: *$p<0.05$, **$p<0.01$, ***$p<0.001$, ns=not significant.

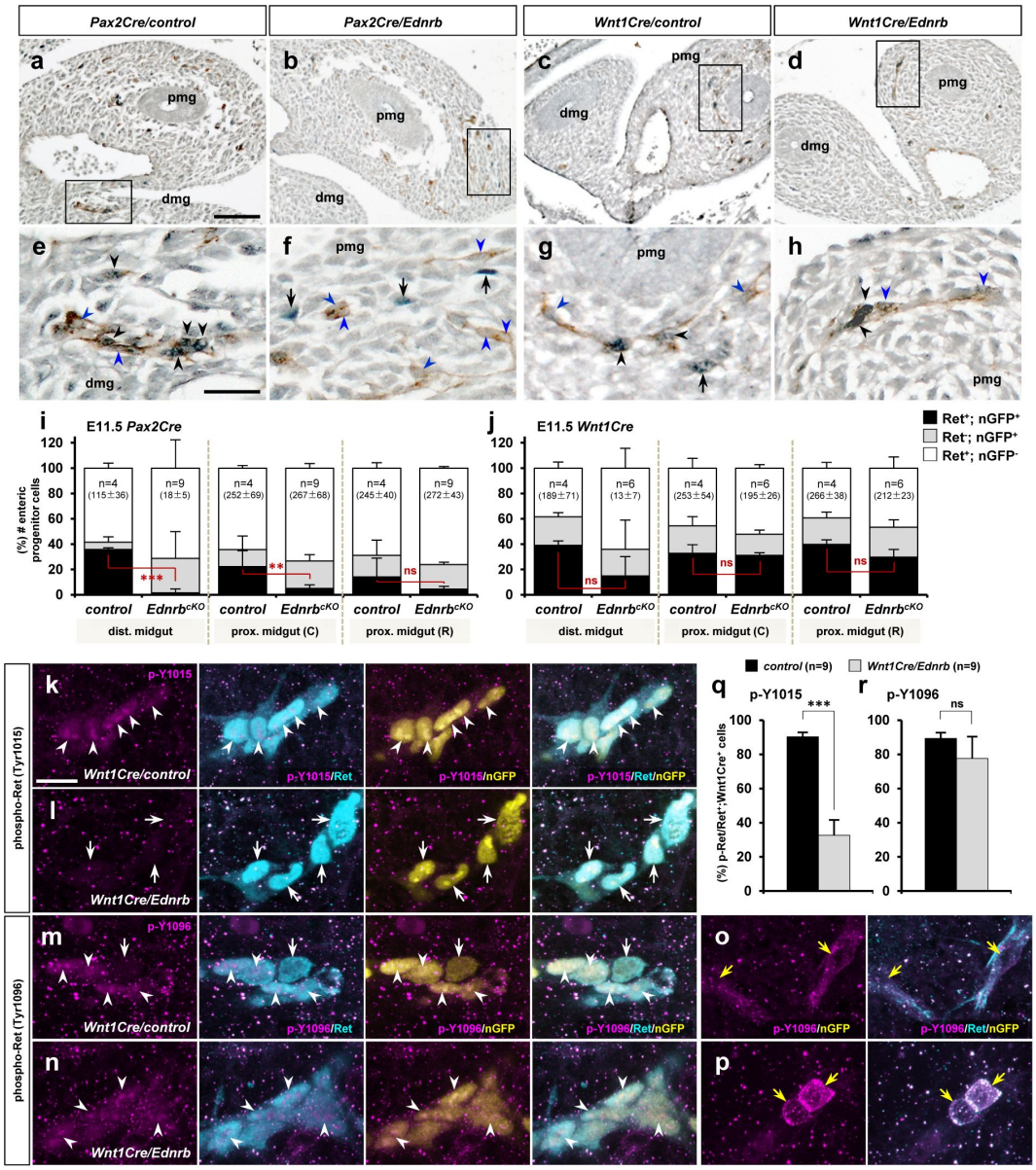

Figure 7.

Lineage selective endothelin-dependent regulation of Ret in migratory ENS progenitor cells.

(a-d) Histological sections showing the apex of the midgut loop of E11.5 *Pax2Cre/Ednrb/R26*$^{nT\text{-}nG}$mutant (b), *Wnt1Cre/Ednrb/R26*$^{nT\text{-}nG}$ mutant (d), and their littermate control embryos (a and c, respectively) stained for nuclear-GFP (blue) and Ret (brown). Magnified views of the bracketed areas (migratory wavefronts) in a-d are shown in e-h, respectively. Abbreviations: dmg, distal midgut; pmg, proximal midgut. **(i-j)** Compiled representations of the fractions of Ret^{+},nGFP^{+} (black); Ret^{-},nGFP^{+} (grey), and Ret^{+},nGFP^{-} (white) ENS progenitor cells in the indicated areas of the embryos of the indicated genotype; (C) and (R) indicate caudal and rostral halves of the proximal midgut. The average total number of countable cells (labeled by either or both markers) in each gut segment is indicated in the parentheses. **(k-p)** Confocal z-stack images of wavefront cells in wholemount preparations of E11.5 guts isolated from *Wnt1Cre/Ednrb/R26*$^{nT\text{-}nG}$ mutants (l,n,p) and their littermate control embryos (k,m,o) stained for nuclear-GFP (yellow), Ret (cyan), and phospho-Ret (Tyr1015) (magenta; k-l) or phospho-Ret(Tyr1096) (magenta; m-p). White arrowheads denote the presence of phosphorylated Ret in the Wnt1Cre-labeled cells, white arrows point to the absence of phosphorylated Ret in the Wnt1Cre-labeled cells, and yellow arrows denote cytoplasmic localization of phosphorylated Ret in nonlineage Ret^{+} cells. **(q-r)** Compiled representations of phospho-Ret-(Tyr1015)$^{+}$ fractions (q) and phospho-Ret-(Tyr1096)$^{+}$ fractions (r) at the wavefront (apex of the midgut loop) in *Wnt1Cre/Ednrb* mutants (n=9; grey bars) and their littermate control embryos (n=9; black bars). P-values: **p<0.05*, ***p<0.01*, ****p<0.001*, ns=not significant. Scale bars, 50μm (a-d), 20μm (e-h, k-p).

have been described for Ednrb to other RTKs (Grantcharova et al., 2006, Harun-Or-Rashid et al., 2016), and Ret with other GPCRs (Tsuchioka et al., 2008). Because Ret expression was preserved in Wnt1Cre-derived enteric progenitors even as they were nonresponsive to GDNF, we considered that transactivation via Ednrb might be involved. To address this, we fluorescently visualized the phosphorylation status of Ret (i.e., its degree of activation) in Wnt1Cre-derived cells in the midgut loop of E11.5 *Wnt1Cre/Ednrb/R26*$^{nT\text{-}nG}$mutants and their littermate embryos. Confocal z-stack images showed that Ret protein was detected in both the cytoplasm and nucleus of Wnt1Cre-labeled migratory cells (**Figure 7k-n**, cyan; nuclear localization of Ret and many other RTKs has been previously noted (Chen and Hung, 2015, Chen et al., 2020) and is not unusual). An antibody specific for phospho-Ret Y1015 was detected in the majority (87%) of control Wnt1Cre-labeled cells (**Figure 7q**), also in the cytoplasm and nucleus (**Figure 7k**, magenta). However, phospho-Y1015 signal was only evident in 33% of *Ednrb*-deficient Wnt1Cre-derived cells (**Figure 7l**, 7q). Thus, a substantial subpopulation of the Wnt1Cre lineage requires Ednrb for Ret Y1015 phosphorylation. Because Ednrb is expressed only in a subset of Wnt1Cre-derived enteric progenitor cells (Figure 7 – figure supplement 1), the residual Y1015 phosphorylation observed in *Wnt1Cre/Ednrb* mutant cells is likely to occur in the Ednrb-negative Wnt1Cre-derived cell population.

Interestingly, *Ednrb*-deficiency did not affect phosphorylation of Ret-Y1096 as demonstrated by positive staining in the Wnt1Cre^{+}; Ret^{+} nuclei (**Figure 7n**, 7r). Furthermore, phospho-Y1096 staining was also notable within the Wnt1Cre-unlabled cell population (nGFP-negative, presumptively of the Pax2Cre lineage), although in these cells, both Ret and phospho-Y1096 Ret showed cell surface rather than nuclear localization (**Figure 7o-p**), suggesting that Ret signaling may be deployed differently in the Pax2Cre lineage. Although we (or other studies) have not yet proven the biological importance of Ret Y1015 in enteric progenitor migration, our results demonstrate that at least one feature of active Ret signaling in Wnt1Cre lineage cells requires the presence of Ednrb.

Discussion

Using the Wnt1Cre and Pax2Cre lines, in this study we have deconstructed the involvement of the two major signaling axes (GDNF/Ret and Edn3/Ednrb) in enteric nervous system development. We have provided new insights on the mechanistic convergence between these signals and on the etiology of Hirschsprung disease.

The ENS has long been thought to derive solely from the neural crest. Our study reveals that the ENS has a dual lineage origin as defined by the Pax2Cre and Wnt1Cre drivers. It is important to clarify that we define these lineages by function (Cre recombination profile) rather than by anatomical origin. It is tempting to assume that these correspond strictly to placode and neural crest, respectively, as they do in craniofacial development (Tan et al., 2023). Nonetheless, for ENS progenitors this is not proven. Thus for example, it is formally possible that these recombination territories for ENS progenitors include different subdomains of neural crest rather than neural crest vs. placode, although even if so this would still fit the definition of dual lineages. For this reason we described the “Pax2Cre lineage” and the “Wnt1Cre lineage” in this manuscript rather than definitively claim these as placode and neural crest. Regardless, we present a compelling argument that these represent at least mostly distinct sublineages of the ENS: their gene expression profiles differ in early progenitor migration, their utilization of GDNF/Ret and Edn3/Ednrb signaling is distinct, the E12.5 consequences of Ret-deficiency in the two lineages are radically distinct, and most importantly at least some of their terminal differentiation fates in the hindgut are unique. These latter two observations also preclude the possibility that Pax2Cre becomes active in migratory Wnt1Cre-derived cells. It is implausible that even a moderate percentage of the Pax2Cre lineage overlaps with the Wnt1Cre lineages: there is no contribution of the Pax2Cre lineage to numerous neural and nonneural structures that receive pre-or post-otic

Wnt1Cre-labeled neural crest cells, and in the mature P9 colon, together the two lineages can account for all Hu^+ neurons (Figure 3 – figure supplement 1g), whereas any appreciable overlap would necessitate a third source of neurons. Our observations support reevaluation of the longstanding dogma of an exclusive neural crest origin of the ENS.

We observed that cells of the Pax2Cre and Wnt1Cre lineages co-mingle in the pharyngeal region and co-migrate through the gut. Indeed our observations indicate that gut migration by each lineage is dependent on the other. We cannot yet explain this behavior. Neural crest cells are known to migrate as an interconnected network, a property called collective cell migration (Theveneau and Mayor, 2012), and it is possible that Pax2Cre-derived cells incorporate into the same. The approx. 15% of cells of both lineages that do not express Ret (**Figure 2v**, grey bars) may also use this mechanism to support their migration. Within this assembly, the different roles of each lineage are unknown. Possible explanations for their required co-dependence could include unique abilities of each to attach to or degrade different components of the matrix, or some sort of paracrine activity that maintains collective migration. The net effect in normal development would be to bring both sets of progenitor cells to the same points of the gut at the same time, which might facilitate terminal assembly of circuitry. This observation of codependent migration might explain in part why the role of the Pax2Cre lineage was never previously recognized: were a subcomponent of the ENS able to migrate normally in neural crest ablation studies, the phenotypic result would likely not be described as aganglionosis.

Defecation is a function that is selectively accomplished by the myenteric plexus of the distal colon, where the integrated circuitry of mechanosensory neurons, excitatory and inhibitory interneurons, and excitatory and inhibitory motor neurons causes what are called “giant migrating contractions” that push fecal material forward (Sarna, 2010). This is a unique neurophysiological process of the distal colon and is distinct from the spontaneous rhythmic contractions that occur with the passage of chyme (partially digested food) along the earlier axis of the gastrointestinal tract. In postnatal mice of each conditional *Ednrb* mutant background, in the proximal colon where cells of both lineages successfully migrate, we observed a selective loss of CGRP mechanosensory neurons in the *Pax2Cre/Ednrb* background, and a selective loss of NOS^+ inhibitory motor neurons in the *Wnt1Cre/Ednrb* background. This observation is informative for demonstrating the developmental potential of each lineage, and corresponds to the fate of each lineage in normal mice, but is representative of only a very specific domain of the mutant guts. The explanation for Hirschsprung disease in both conditional *Ednrb* mutants is the total deficiency of both lineages in the distal colon, combined with the selective loss of specific neuronal subtypes in the transition zones (Figure 3 – figure supplement 3) immediately prior to the aganglionic areas.

Using *Ret* conditional knockout, we observed that the Wnt1Cre and Pax2Cre lineages differ significantly in their use of GDNF signaling. Thus, the Wnt1Cre lineage requires GDNF responsiveness to migrate past the stomach, whereas the Pax2Cre lineage migrated into the midgut and only became GDNF-dependent at the hindgut. This behavior corresponds to expression of Ret in the early stages of Wnt1Cre-derived cells, and later abundance of Ret expression in Pax2Cre-derived cells. Alternative factors present in the foregut may uniquely support migration of the Pax2Cre lineage, but other explanations are possible.

Our studies demonstrate that Edn3 signaling through Ednrb is required to support GDNF responsiveness and thereby to support cell migration in both the Pax2Cre and Wnt1Cre lineages. We describe independent mechanisms to explain this relationship: Ret expression is induced or expanded by Ednrb signaling in Pax2Cre-derived cells, whereas in Wnt1Cre-derived cells, Ednrb induces competence for Ret signaling without changing Ret expression. It should be clear that we have not yet proven that either role is functionally required for normal ENS development, so for the present these are still candidate mechanisms. Regarding the latter, we determined that phosphorylation of Ret Y1015 requires Ednrb activity in Wnt1Cre-derived cells. Phosphorylation of this residue is known to activate the PLCg/PKC pathway (Mahato and Sidorova, 2020). For

practical reasons, in this study we only investigated phospho-Y1015 and phospho-Y1096, and other modification sites or types might be more relevant to explain the relation between Ednrb and Ret in enteric progenitors of the Wnt1Cre lineage. In any event, the conceptual conclusion that Edn3-Ednrb signaling converges on GDNF-Ret function in both the Pax2Cre and Wnt1Cre lineages is supported by both the in vitro and in vivo observations and helps to explain the common phenotype of Hirschsprung disease that is seen when any component is mutated.

Our analyses have delineated the dual lineage origins of $CGRP^+$ mechanosensory and NOS^+ inhibitory motor neurons of the distal colonic circuitry, but clearly there is vastly more complexity in the ENS that is yet to be understood. Myenteric ganglia contain additional neural and glial subtypes that are still uncharacterized for lineage origin and function. Furthermore, the small intestine and proximal colon have their own physiology and functions, and it is expected that the ENS sustains the autonomy of these components of the gut through additional specialized circuits that respond to appropriate stimuli and execute different commands from those in the distal colon. As Wnt1Cre-derived and Pax2Cre-derived cells both colonize the foregut and midgut as well as the hindgut, we speculate that each lineage may also be allocated to distinct fates and functions in order to complete a functional circuitry in these parts of the gut.

We were able to define the distinct contributions of the Wnt1Cre and Pax2Cre lineages to the ENS using appropriate genetic strategies in mice. Cell-based transplantation approaches to restore bowel function in Hirschsprung disease infants are currently focused only on neural crest cells, for example as derived by directed differentiation from pluripotent stem cells. To fully reconstitute a functional ENS circuitry in patients, it will be necessary to ensure that these transplanted cells have the capacity to differentiate into the full range of ENS cell types, including mechanosensory neurons.

With the same null mutation of *Ednrb*, the severity of Hirschsprung disease is highly dependent on strain background in rats (Dang et al., 2011) and mice (Hosoda et al., 1994). This indicates the existence of unlinked alleles that modify the consequences of *Ednrb*-deficiency. Similarly, in humans, Hirschsprung disease-associated mutations are almost always heterozygous (presumably haploinsufficient), but show variable extent of phenotypic penetrance, even so far as to be inherited in some affected patients from one asymptomatic parent (Fuchs et al., 2001). In some cases, the genetic background effect involves a mutation in a gene already known to be associated with Hirschsprung disease: a human genome-wide association study demonstrated genetic interaction between the *EDNRB* and *RET* loci (Carrasquillo et al., 2002), and synergy was evident in mice with intentional combinations of *Ednrb* and *Ret* (McCallion et al., 2003) or *Ednrb* and *Sox10* (Cantrell et al., 2004) alleles. Clearly there is opportunity to discover new genes that do not independently cause Hirschsprung disease but which modify the penetrance of the known set of genes. In this light, it was striking that mice on an ICR background with conditional or global *Ednrb* deficiency die consistently around 3 weeks of age. ICR mice are an outbred background with a genetic mixture of many poorly characterized ancestral sources (Aldinger et al., 2009) and have been maintained as an internally crossed (but not inbred) breeding colony by many providers.

Interestingly, in congenital sensorineural deafness, the other major EDN3-EDNRB phenotype that with Hirschsprung disease defines Waardenburg-Shah syndrome type IV, the penetrance of hearing impairment in ICR-background Edn3 or *Ednrb* mutant mice is variable (approx. 50%)(Tan et al., 2023). This indicates that different modifiers interact with Edn3-Ednrb in auditory development vs. enteric nervous system development. These mouse models may help to clarify the additional components and downstream pathways that result in human Hirschsprung and Waardenburg-Shah pathologies.

Materials and methods

Animals

Ednrb (Rattner et al., 2013) (JAX:011080), *Edn3* (Baynash et al., 1994) (JAX:002516), *Ret* (Luo et al., 2007) (JAX:028548), *Pax2Cre* (Ohyama and Groves, 2004), *Wnt1Cre* (Danielian et al., 1998), $ROSA26^{lacZ}$ (Soriano, 1999), $ROSA26^{CAG\text{-}tdTomato}$ (Madisen et al., 2010) (JAX: 007914), $ROSA26^{nT\text{-}nG}$ (Prigge et al., 2013) (JAX: 023537),

$ROSA26^{EYFP}$ (Srinivas et al., 2001) (JAX:006148), *Ednrb-EGFP* (Gong et al., 2007) (MMRRC_010620-UCD) alleles have been described previously. Wild-type ICR mice used for propagation of these lines were obtained from Harlan/Envigo. All alleles used in this study have been backcrossed for numerous generations to the ICR background, although because of intercrosses this was not rigorously controlled or quantified. All experiments with animals complied with National Institutes of Health guidelines and were reviewed and approved by the Medical University of South Carolina Institutional Animal Care and Use Committee.

24-hour fecal collection

2.5-week-old animals were individually housed in a single mouse metabolic cage (Tecniplast) for 24 hours. Feces collected in a collection funnel were dried and measured for their dry weight.

Postnatal distal colon preparation

Postnatal day 9 mice were anesthetized and transcardially perfused with PBS, and then the entire colon (including proximal colon) was dissected and transferred to PBS. After removing fecal materials by flushing PBS through the colon, a glass capillary tube was inserted to straighten the colon, and the colon was then fixed in an appropriate fixative at 4°C overnight. Fixatives used in this study were glutaraldehyde (0.2% glutaraldehyde, 0.4% paraformaldehyde, 2mM $MgCl_2$ in PBS) for X-gal staining, and paraformaldehyde (4% PFA in PBS) for immunofluorescence staining.

Wholemount Xgal staining

Fixed embryos, embryonic gut tissues and postnatal colon preparations were washed with detergent rinse (0.02% NP40, 0.01% sodium deoxycholate, 2mM $MgCl_2$ in PBS), and stained with Xgal staining solution (1mg/ml Xgal in 0.1M TrisHCl pH=7.4, 2mM $MgCl_2$, 0.02% NP40, 0.01% sodium deoxycholate, 5mM $K_3[Fe(CN)_6]$, 5mM $K_4[Fe(CN)_6]$ in PBS) at room temperature overnight. The colon was opened by longitudinal incision, the (inner) submucosal and mucosal layers were removed, and the outer tissue (containing circular muscle, the myenteric plexus, longitudinal muscle, and serosa) was stained. Xgal stained tissues were washed with PBS, and either or then used for *in situ* hybridization or wholemount immunostaining.

In situ hybridization

Xgal stained embryonic gut tissues were washed with PBST (1% Tween-20 in PBS), dehydrated in a methanol series ultimately to 100% methanol, then bleached in 3% H_2O_2 in methanol for 20 min at room temperature. Tissues were rehydrated in PBST, digested with 10µg/ml Proteinase K in PBST for 4 min at room temperature, and then washed in 2mg/ml glycine containing PBST. After post-fixation with 4% PFA for 10 min at room temperature, tissues were washed with PBST, equilibrated with hybridization solution (50% formamide, 5xSSC pH=4.5, 1% SDS, 50µg/ml yeast tRNA, 50µg/ml heparin), and incubated with biotin-labeled RNA probe at 70°C overnight. Tissues were then washed with hybridization solution (without yeast tRNA and heparin) three times at

70°C, three times with high stringent wash (50% Formamide, 2xSSC pH=4.5) at 65°C, and washed with PBST at room temperature. Biotinylated-probe was then detected by Streptavidin-HRP antibody followed by DAB chromogen reaction (see wholemount immunostaining below).

Frozen sections were prepared from fixed embryos that were cryoprotected in 30% sucrose in PBS followed by embedding in OCT compound. Sections were post-fixed for 10 min in 4% PFA/PBS, washed with PBST, and then acetylated in 0.25% acetic anhydride containing 0.1M triethanolamine for 5 min at room temperature. Section were equilibrated with hybridization solution (50% formamide, 5xSSC pH=4.5, 50µg/ml yeast tRNA), and incubated with DIG-labeled RNA probe at 58°C overnight. Sections were then washed with hybridization solution (without yeast tRNA) at 58°C, 2xSSC at room temperature, 2xSSC at 65°C, and followed by 0.1xSSC at 65°C. After wash with TBST (0.1% Tween-20 in TBS), DIG-labeled probe was detected by Alkaline phosphatase conjugated DIG antibody followed by NBT/BCIP reaction in NTMT (0.1M NaCl, 0.1M TrisHCl pH=9.5, 50mM $MgCl_2$, 0.1% Tween-20) with 2mM levamisole. *In situ* labeled sections were then subjected to immunofluorescence staining (see immunofluorescence staining below). Riboprobes for *Edn3* and *Ednrb* genes are described previously (Makita et al., 2008).

2-color immunohistochemistry

5µm continuous paraffin sections prepared from the head to tail of E10.5-12.5 *Pax2Cre/Ret/R26*$^{nT\text{-}nG}$, *Pax2Cre/Ednrb/R26*$^{nT\text{-}nG}$, *WntCre/Ret/R26*$^{nT\text{-}nG}$, *Wnt1Cre/Ednrb/R26*$^{nT\text{-}nG}$, and their littermate control embryos were deparaffinized in xylene, rehydrated through an ethanol sequence, and then microwaved for 25 min in citrate buffer (10mM sodium citrate pH=6.0) for antigen retrieval. Histological slides were bleached in 3% H_2O_2 in methanol for 2 min, washed in PBST (0.1% Tween-20 in PBS), and then first incubated with chicken anti-GFP antibody (1:3000, Abcam ab13970) at 4°C overnight. After three washes with PBST, sections were incubated with HRP conjugated anti-chicken-IgY (1:200, Jackson ImmunoResearch 703-035-155) for 2-3 hr at room temperature. GFP signal was then detected by 0.5mg/ml DAB-blue solution containing 0.05% $CoCl_2$, 0.05% $Ni(NH_4)_2(SO_4)_2$ (pH=7.2) with 0.015% H_2O_2. Nuclear-GFP immunolabeled sections were then bleached in 3% H_2O_2 in methanol for 2 min, washed in PBST (0.1% Tween-20 in PBS), and incubated with goat anti-Ret antibody (1:300, R&D Systems AF482) at 4°C overnight. After incubating with HRP-conjugated goat-IgG secondary antibody, Ret signal was detected using DAB-brown solution (0.5mg/ml DAB with 0.03% H_2O_2). Slides were washed in ddH_2O, dehydrated in an ethanol sequence followed by xylene and mounted with DPX medium.

All sections containing foregut through midgut areas containing immunolabeled cells were captured as digital images using a Nikon DS-Fi1 digital camera in continuous order. For E10.5 analysis (**Figure 2v-x**), nGFP-positive, Ret-positive, and nGFP and Ret-double positive cells in the midgut segments were counted in every third section (15µm intervals to avoid counting the same cell twice) using Fiji ImageJ plugin Cell Counter. For E11.5 analysis, nGFP-positive, Ret-positive, and nGFP and Ret-double positive cells in the rostral and caudal halves of the proximal midgut and in the distal midgut segments were counted separately in every third section (15µm intervals to avoid counting the same cell twice), and compiled as whole midgut cell counts for lineage specific Ret mutants (**Figure 2y-z**) or as cell counts of each segment for lineage specific Ednrb mutants (**Figure 7i-j**).

Embryonic gut slice preparation for collagen gel explant culture

Tomato$^+$ embryos from *Pax2Cre/Ret/R26*$^{td\text{-}Tomato}$, *Pax2Cre/Ednrb/R26*$^{td\text{-}Tomato}$, *WntCre/Ret/R26*$^{td\text{-}Tomato}$, *Wnt1Cre/Ednrb/R26*$^{td\text{-}Tomato}$ and their littermate control embryos were collected in PBS under a fluorescence dissection scope (Nikon SMZ800), and midgut segments were dissected in PBS as described in Figure 5 – figure supplement 1. For E10.5 explants, dissected midgut segments were embedded in 6% low melt agarose in PBS, and sectioned transversely from the caudal to rostral direction using a Vibratome 1000 microtome. Each 200µm section was placed in a culture medium droplet on petri dish and these were maintained in their caudal to rostral order until

explanted in collagen gel. For E11.5 explants, both proximal and distal midgut segments were separately embedded in 6% low melt agarose in PBS, sectioned in a caudal to rostral and rostral to caudal direction, respectively, and placed in culture media droplets prior to explanting in collagen gel. To ensure similar stages of development between different litters, E10.5 tissue sections were only used if the midgut was 1.0-1.4mm, and for E11.5 tissue if the proximal midgut segments was 1.6-2.0mm.

Collagen gel explant culture

Rat tail collagen and collagen gel preparation were performed as previously described (Guthrie and Lumsden, 1994) with minor modifications. Briefly, rat tail collagen was prepared by dissolving 2.5mg/ml rat tail tendons in 0.5N acetic acid at 4°C for two days. The solution was then centrifuged at 12,000rpm for 1 hr at 4°C to remove debris, and the supernatant dialyzed against 0.1X Basal Eagle's Medium (BME) for 3 days at 4°C. For collagen gel explant culture, 4XBME and 7.5% sodium bicarbonate (with or without growth factor, see below) were gently placed into dialyzed rat tail collagen solution on ice to a final concentration of 1X and 0.2%, respectively. After very gentle pipetting up and down on ice, 25ul collagen drops were placed onto a Petri dish, and then flattened by gently dropping the dish onto a flat surface several times. The collagen beds were then solidified in a tissue culture incubator (5% CO_2, 37°C) for 10 min. Once the collagen beds solidified into a gel, each embryonic gut slice was placed onto a collagen bed and mounted with 40ul of freshly prepared collagen solution (1XBME, 0.2% $NaHCO_3$, with or without growth factor in dialyzed collagen), and the dish returned to the incubator for 10 min. Once the top collagen was fully solidified, culture medium with or without growth factor was added to the Petri dish to fully submerge the collagen gel domes. Gut slice explants were then cultured in 5% CO_2 at 37°C for 3 days. Culture media used was DMEM supplemented with 10% FBS, 100U/ml penicillin/streptomycin, 100µM putrescine (Sigma-Aldrich P5780), 10ng/ml progesterone (Sigma-Aldrich P7556), 200ng/ml selenious acid (Sigma-Aldrich 211176), 500µM sodium butyrate (Sigma-Aldrich B5887), 1mM sodium pyruvate (Sigma-Aldrich P2256), 5µg/ml transferrin (Sigma-Aldrich T8158), 2ng/ml triiodo-L-thyronine (T3) (Sigma-Aldrich T6397). Growth factors used were recombinant mouse GDNF (10ng/ml, Abcam ab 56286), endothelin-3 (10nM, Enzo LifeSciences ALX-155-003) and recombinant mouse NGF (10ng/ml, Sino Biological 50385-MNAC). This EDN3 concentration promotes neurite outgrowth from embryonic sympathetic and CNX ganglion explants (Makita et al., 2008) and NGF at the utilized concentration is widely used to promote growth and survival of variety of neuronal types (Kuruvilla et al., 2004). After 3 days, the Petri dishes containing the collagen gel domes were fixed in 4% PFA for 2 hr at 4°C and washed with PBS. The explanted tissue morphology and its Tomato$^+$ cell profiles were recorded in continuous axial order under bright field and epifluorescence settings, respectively (Nikon Eclipse 80i upright microscope). The collagen domes were then gently peeled off from the Petri dish and wholemount immunofluorescence stained (see immunofluorescence staining below) for confocal imaging. Total Tomato$^+$ outgrowth area was measured from epifluorescence images acquired from a Nikon Eclipse 80i upright microscope using Fiji Image J software; binary threshold selection of the Tomato$^+$ area of the original explanted tissue was subtracted from the terminal Tomato$^+$ area. For both E10.5 and E11.5 stages, the outgrowths of 6 sections (0-1200µm range, see Figure 5 – figure supplement 1) from each midgut segments were compiled into the dot plots. If individual explanted slices failed to stay in the collagen gel their individual data were not included in the analysis.

Wholemount immunostaining

Fixed tissues (mouse embryos, embryonic guts, postnatal gut slices, postnatal distal colon preparations) were dehydrated in a methanol series (to 100%), and bleached overnight in 3% H_2O_2 in 20% DMSO containing methanol solution. Tissues were then rehydrated in PBST (1% Tween-20 in PBST), and incubated in blocking solution (1% non-fat dried milk, 20% DMSO in PBST) for 10-60 min at room temperature followed by incubation with primary antibody in blocking solution for 2-3 days at 4°C. After extensive washes with PBST, tissues were incubated with HRP-conjugated

secondary antibody (1:200, Jackson Immunoresearch) for 2-3 days at 4°C. Immunoreactive signal was then visualized by DAB detection (0.2mg/ml DAB in PBST with 0.03% H_2O_2). Stained tissues were cleared with Sca*l*eU2 (4M urea, 30% glycerol, 0.1% Triton-X 100) for imaging. Antibodies used included rabbit anti-Pax2 (1:50, Invitrogen 08-1483), rabbit anti-AP2 (1:1000, Abcam ab52222), goat anti-Sox10 (1:200, Santa Cruz sc-17342), mouse anti-HuD (1:500, Santa Cruz sc-13577), mouse anti-Tuj1 (1:1000, Biolegend MMS-435P), rabbit anti-CGRP (1:500-1000, Millipore PC205L), and rabbit anti-NOS1 (1:500, Santa Cruz sc-648). Stained tissues were cleared with Sca*l*eU2 and flat-mounted to histology slides for imaging. $CGRP^+$ afferent projections in colonic mucosa were quantified by binary threshold-level selection of the $CGRP^+$ pixel area per single villus and NOS^+ efferent projections were also quantified by binary threshold-level selection of NOS^+ pixel area in the circular muscle layer, both using Fiji-Image J software.

Wholemount immunofluorescence staining

Fixed tissues (embryonic vibratome sections, embryonic gut tissues, collagen gel cultured explants, postnatal colon vibratome sections and preparations) were permeabilized in PBST (1% Tween-20 in PBS), incubated in blocking solution (1% non-fat dried milk, 20% DMSO in PBST) for 10-60 min at room temperature followed by incubation with primary antibody in blocking solution for 2-3 days at 4°C. After extensive washing with PBST, tissues were incubated with Alexa Fluor-conjugated secondary antibody (1:500, Invitrogen) for 2-3 days at 4°C. Immunolabeled tissues were counterstained with DAPI and cleared with Sca*l*eU2 and mounted to histology slides for confocal imaging. Antibodies used were rabbit anti-Pax2 (1:50, Invitrogen 08-1483), rabbit anti-AP2 (1:1000, Abcam ab52222), goat anti-Sox10 (1:200, Santa Cruz sc-17342), mouse anti-2H3 (1:100, DSHB), chicken anti-GFP (1:3000, Abcam ab13970), goat anti-p75 (1:300, R&D systems AF1157), mouse anti-HuD (1:500, Santa Cruz sc-13577), rabbit anti-BLBP (1:500, Abcam ab32423), mouse anti-Tuj1 (1:1000, Biolegend MMS-435P), rabbit anti-CGRP (1:500-1000, Millipore PC205L), rabbit anti-NOS1 (1:500, Santa Cruz sc-648), goat anti-Ret (1:300, R&D Systems AF482), rabbit anti-phospho-Ret (Tyr1015) (1:300, ThemoFisher PA5-105930) and rabbit anti-phospho-Ret (Tyr1096) (1:300, ThemoFisher PA5-105796). Fiji Image J plugin cell counter was used for counting $Tomato^+$, $CGRP^+$, NOS^+, GFP^+, and Hu^+ ganglion cells in myenteric plexuses of the distal colon (defined on the basis of perfusion by the inferior mesenteric artery), and for counting Ret^+, phospho-Ret $Tyr1015^+$, phospho-Ret $Tyr1096^+$, and GFP^+ cells in E11.5 embryonic ENS wavefront cells.

Statistics

All quantified data were graphed as mean±SEM, and analyzed for significance using a two-tailed Student's t-test. Dot plots show the each individual data points and mean.

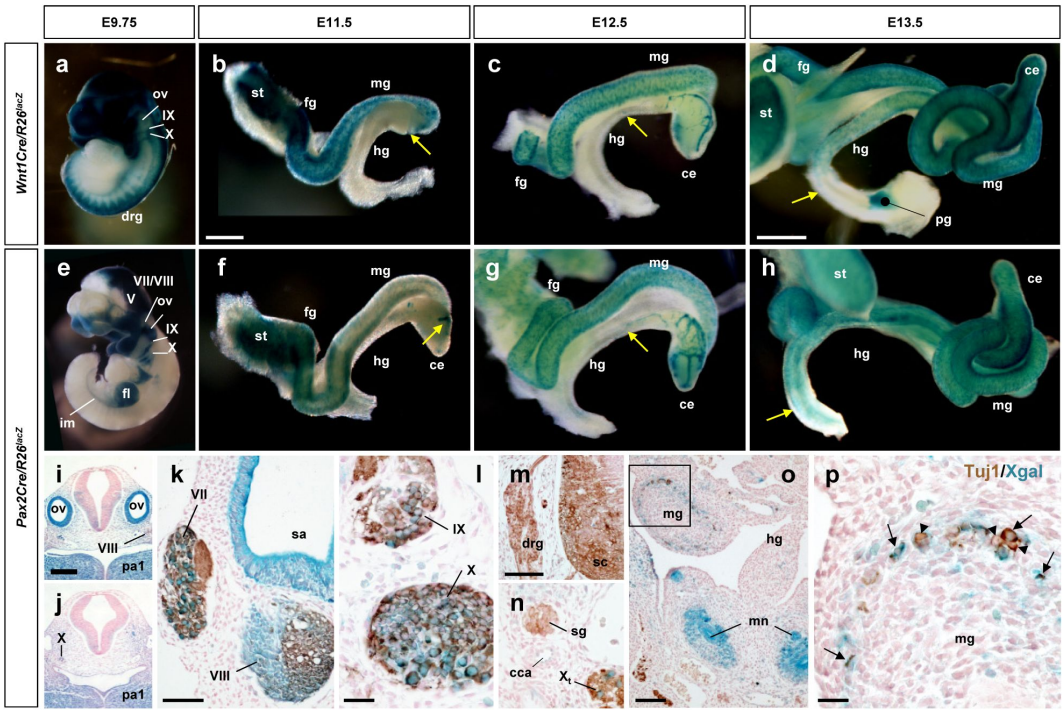

Figure 1 – figure supplement 1.

Pax2Cre-derived cells contribute to the ENS.

(a-h) Wnt1Cre– and Pax2Cre-lineage tracing in developing gut. Wholemount X-gal staining of *Wnt1Cre/R26*^{lacZ} (a) and *Pax2Cre/R26*^{lacZ} (e) embryos at E9.75. Wholemount X-gal stained guts isolated from *Wnt1Cre/R26*^{lacZ}(b-d) and *Pax2Cre/R26*^{lacZ} (f-h) embryos at E11.5 (b, f), E12.5 (c, g) and E13.5 (d, h). Arrows denote migrating wavefronts of Wnt1Cre-labeled (b-d) and Pax2Cre-labeled (f-h) cells on the gut walls. (i-j) Transverse sections of the hindbrain region of a *Pax2Cre/R26*^{lacZ}embryo at E9.5. (k-p) Transverse sections of E12.5 *Pax2Cre/R26*^{lacZ} embryos immunolabeled for Tuj1 (brown). Pax2Cre labels the inner ear (sa, which is otic placode-derived and non-neurogenic), and also subsets of CN V, VII, VIII, IX and X neurons (epibranchial placode-derived) (k-l), and the metanephros (o), but does not label dorsal root (m) or sympathetic ganglion (n) neurons which originate exclusively from trunk neural crest cells. Magnified view of bracketed area in o is shown in (p); arrows in (p) denote Pax2Cre-labeled Tuj1^{+} ENS neurons. Arrowheads point to Pax2Cre-unlabeled neurons. Abbreviations: cca, common carotid artery; ce, cecum; drg, dorsal root ganglion; fg, foregut; hg, hindgut; mn, metanephros; mg, midgut; ov, otic vesicle; pa, pharyngeal arch; pg, pelvic ganglion; sa, saccule; sc, spinal cord; sg, sympathetic ganglion; st, stomach. V, fifth (trigeminal) ganglion; VII, seventh (facial/geniculate) ganglion; VIII, eighth (vestibulocchlear) ganglion; IX, ninth (glossopharngeal/petrosal) ganglion; X, tenth (vagus/nodose) ganglion. Scale bars, 500μm (b-c, f-g, g-k), 1000μm (d, h), 200μm (i-j), 100μm (k, m-n, o), 25μm (l, p).

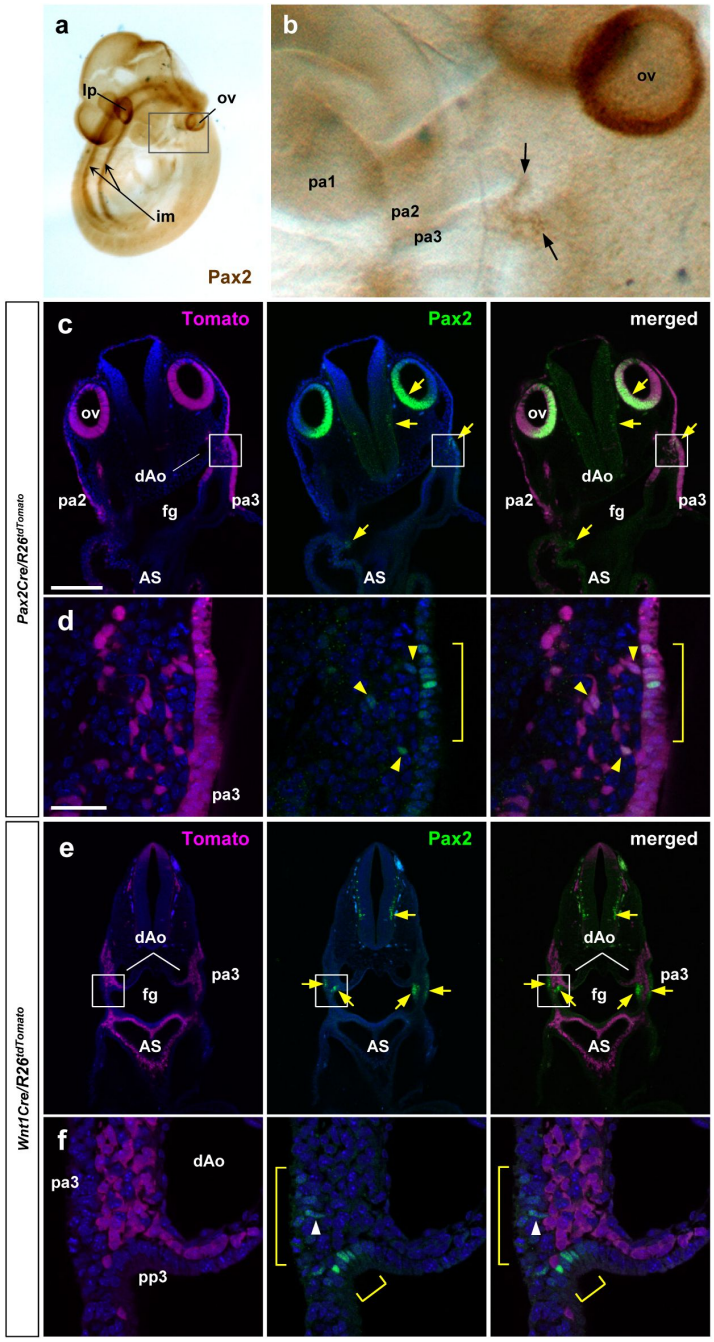

Figure 1 – figure supplement 2.

Pax2Cre and Wnt1Cre label distinct early migratory cell populations.

(a-b) An E9.5 wild-type embryo immunostained for Pax2 protein; (b) is a magnified view of the bracketed area including the pharyngeal arch regions in a. Arrows denote Pax2-expressing cells of the third pharyngeal cleft and pouch. (c-f) Vibratome sections of E9.75 *Pax2Cre/R26*^{tdTomato} (c-d) and *Wnt1Cre/R26*^{tdTomato}(e-f) embryos immunostained for Pax2. Yellow arrows denote Pax2 expression (c, e). Magnified views of bracketed area of c and e are shown in d and f. Yellow brackets denote the Pax2 expressing cells in the third pharyngeal ectoderm and endoderm (d, f). Yellow arrowheads point to Pax2-expressing Pax2Cre^{+} cells that are delaminated and migrating from the ectodermal layer (d). White arrowhead points to a Pax2-expressing Wnt1Cre-unlabeled cell that has just delaminated from the ectoderm (f). Abbreviations: AS, aortic sac; dAo, dorsal aorta; im, intermediate mesoderm; lp, lens placode; pa, pharyngeal arch; pp, pharyngeal pouch. Scale bars, 200μm (c,e), 25μm (d,f).

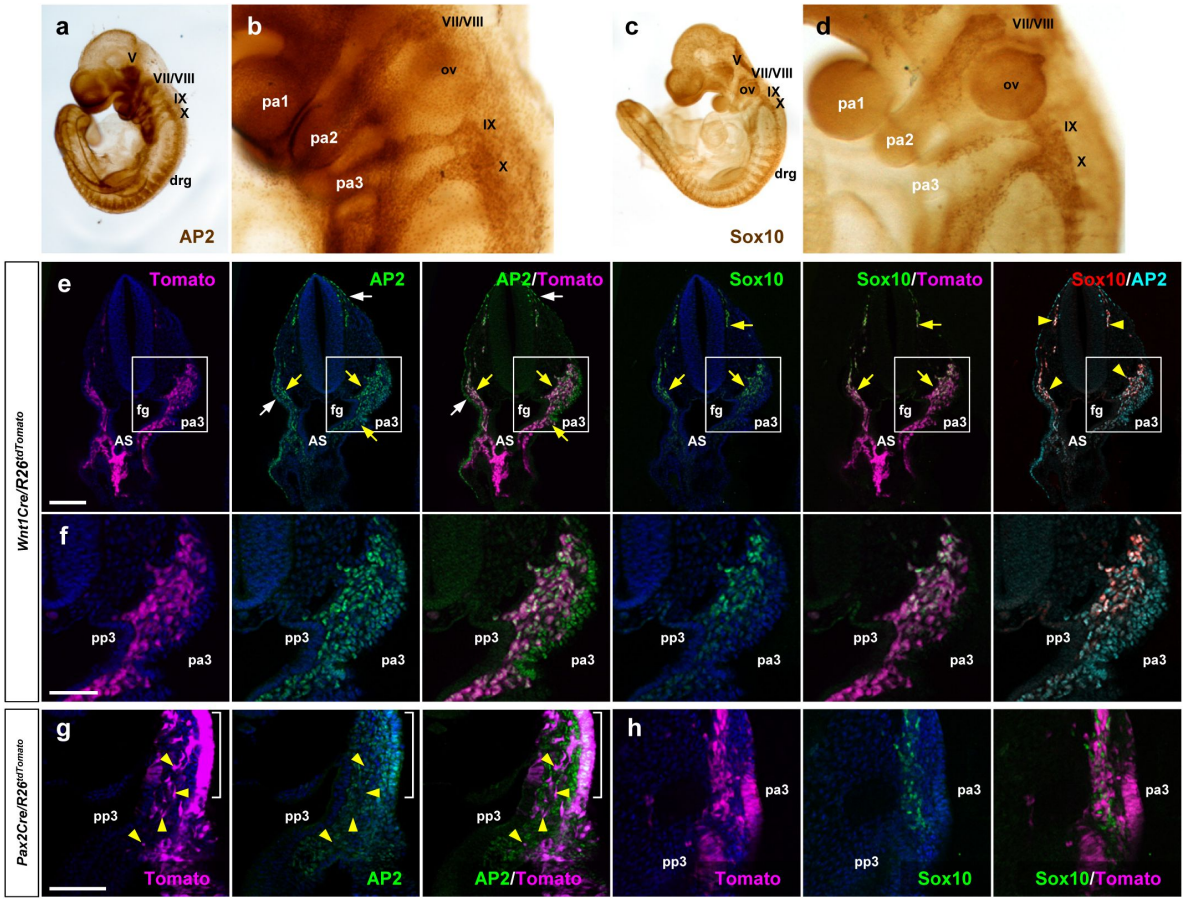

Figure 1 – figure supplement 3.

Distinct lineage origin of Pax2Cre-labeled and Wnt1Cre-labeled ENS progenitor cells.

(a-d) E9.5 wild-type embryos stained for AP2 (a-b) and Sox10 (c-d). Magnified views of the bracketed areas including the pharyngeal arch regions in a and c are shown in b and d, respectively. (e-f) Vibratome sections of E9.75 *Wnt1Cre/R26*^{tdTomato}embryo immunostained for AP2 and Sox10. White arrows denote AP2^{+} ectodermal cells. Yellow arrows indicate the Wnt1Cre-labeled neural crest cell population expressing AP2 or Sox10. Magnified views of the bracketed areas in e are shown in f. (g-h) Magnified views of vibratome sections of E9.75 *Pax2Cre/R26*^{tdTomato} embryo immunostained for AP2 (g) or Sox10 (h). Yellow arrowheads point to migratory Pax2Cre-derived cells with AP2-negative nuclei. Scale bars, 200μm (e), 100μm (f-h).

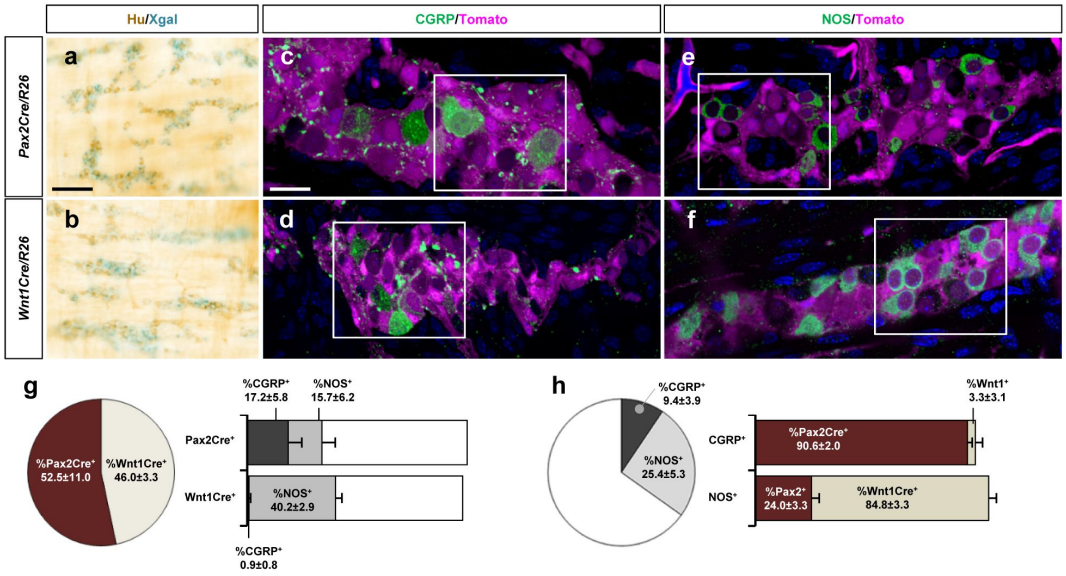

Figure 3 – figure supplement 1.

Pax2Cre-derived cells preferentially give rise to CGRP$^+$ myenteric neurons of the distal colon.

(a-b) Wholemount preparations of P9 distal colons isolated from *Pax2Cre/R26^{lacZ}* (a) and *Wnt1Cre/R26^{lacZ}* (b) mice were Xgal stained and immunolabeled for Hu (a-b). (c-f) Wholemount preparations of P9 distal colons isolated from *Pax2Cre/R26^{tdTomato}*(c,e) and *Wnt1Cre/R26^{tdTomato}* (d,f) were immunofluorescence labeled for CGRP (c,d) or NOS (e,f) and counterstained by DAPI. Magnified views of bracketed areas in c-f are shown in **Figure 3 d-g**. (g,h) Compiled representations of the proportion of Pax2Cre$^+$ and Wnt1Cre$^+$ neurons (g) or the proportion of CGRP$^+$ and NOS$^+$ neurons (h) among a total of 5585 myenteric neurons counted from the P9 distal colons isolated from 9 *Pax2Cre/R26^{tdTomato}* and 8 *Wnt1Cre/R26^{tdTomato}*mice (mean±s.e.m). The proportion of the CGRP$^+$ and NOS$^+$ neurons within the Pax2Cre$^+$ or the Wnt1Cre$^+$ population are presented in the bar graph of (g). The percentage of Pax2Cre$^+$ and Wnt1Cre$^+$ neurons in the CGRP$^+$ or NOS$^+$ populations are shown in the bar graph of (h). The pie charts and bar graphs do not add to 100% because these are compiled from separate and independent measurements that were compiled together graphically for ease of comparison. Error bars, mean±s.e.m. Scale bars, 100μm (a-b), 20μm (c-f).

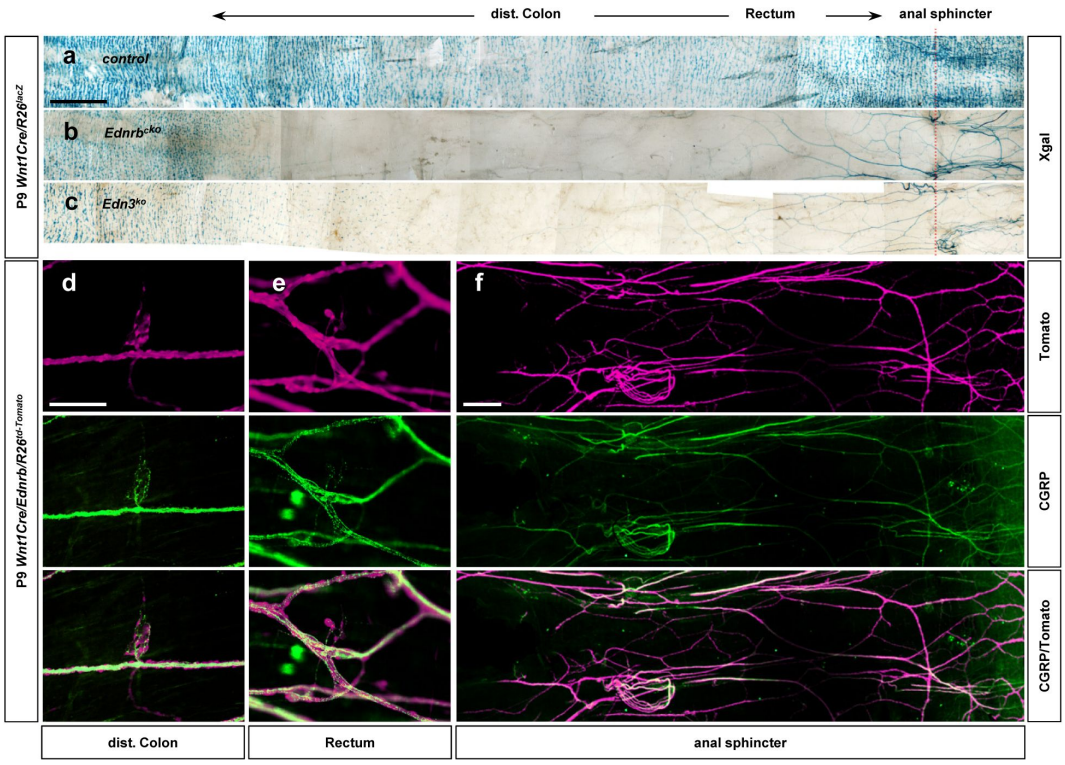

Figure 3 – figure supplement 2.

Pelvic ganglion neurons and their projections express CGRP.

(a-c) Distal-most end of Xgal-stained colons of the control (a), *Wnt1Cre/Ednrb* (b), and global *Edn3* (c) mutants shown in **Figure 1l-n**, respectively. In the absence of vagal neural crest-derived intrinsic ENS ganglia (b-c), sacral neural crest-derived pelvic ganglia and their axons become noticeable with Xgal staining. (d-f) Epiflurorecence microscope images of wholemount preparations of the distal colons isolated from P9 *Wnt1Cre/Ednrb/R26*$^{td\text{-}Tomato}$ mutant immunofluorescently labeled for CGRP shows sacral neural crest-derived CGPR^{+} neurons and axons in the distal colon (d), rectum (e) and anal sphincter (f) areas. Scale bars, 1000μm (a-c), 100 μm (d-e), 500 μm (f).

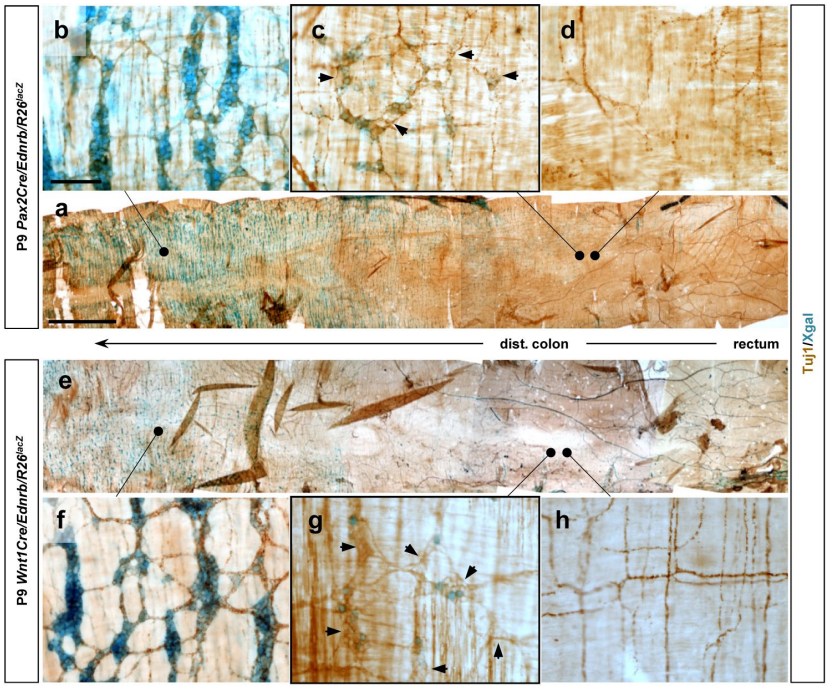

Figure 3 – figure supplement 3.

Transition areas in lineage-specific *Ednrb* mutant distal colon also contain lineage-unlabeled neurons.

(a,e) Wholemount preparations of P9 distal colons isolated from *Pax2Cre/Ednrb* (a) and *Wnt1Cre/Ednrb* (e) stained with Xgal and for Tuj1 to visualize lineage-labeled and lineage-unlabeled neurons and their axons. (b-c,f-h) Magnified views showing myenteric plexus morphology in the areas that are normally colonized (b,f), at the location of terminal migration (c,g), and at a location immediately beyond the point of terminal migration (d,h). Residual Tuj1 signal in axons in d and h are extrinsic nerves. Histological analysis for CGRP and NOS in **Figure 3h-o** was performed with segments equivalent to the location of panels c and g. Arrows in c and g point to lineage-unlabeled cells of myenteric ganglia. Scale bars, 1000μm (a, e), 100μm (b-d, f-h).

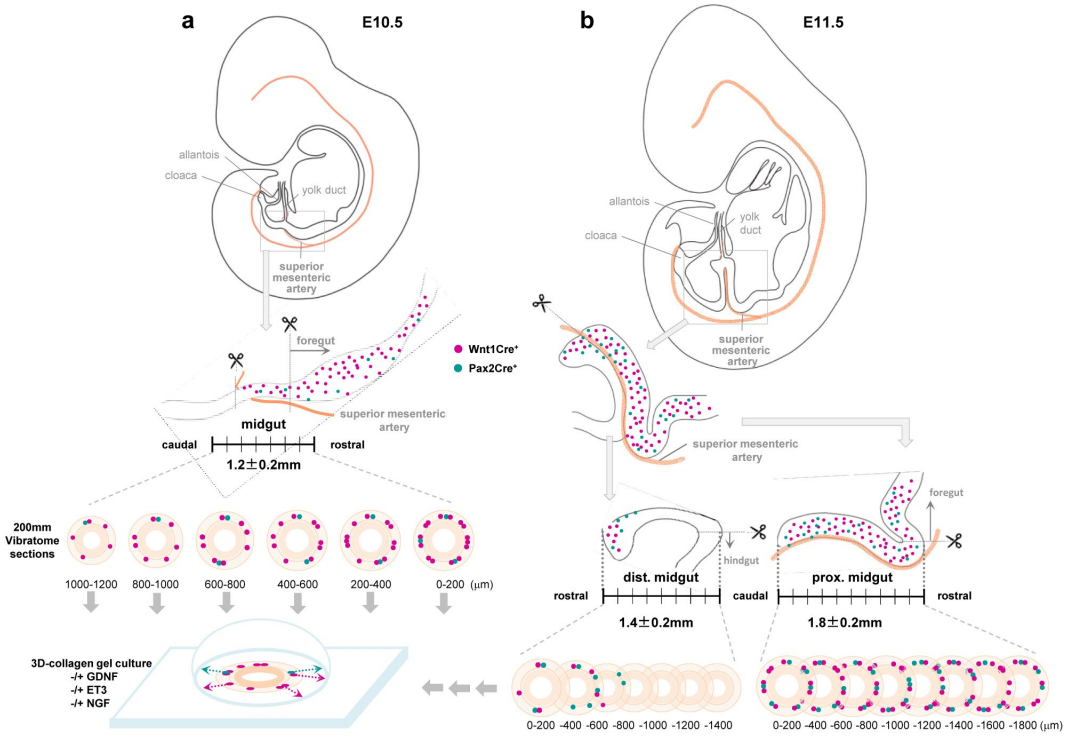

Figure 5 – figure supplement 1.

Schematic illustrations of rostrocaudal orientation of gut slice explant culture.

(a) E10.5 midgut slice preparation. The midgut segment was isolated based on the origin of the superior mesenteric artery from the dorsal aorta (cranial end) to where it meets the yolk (vitelline) duct. 200μm vibratome sections were prepared in a rostral to caudal direction and individually cultured in collagen gel in the absence or presence of GDNF, EDN3 or NGF. (b) E11.5 midgut slice preparation. First, the whole gut tissue (from stomach through cloaca) was excised from E11.5 embryo, and then the midgut loop was isolated. The proximal midgut segment was dissected by separating the midgut loop along the superior mesenteric artery and then by removing the foregut portion at the cranial end of the superior mesenteric artery. The superior mesenteric artery was kept with the proximal midgut segment for the rest of the procedure. The hindgut was then removed from the distal midgut segment based on the position of the inferior mesenteric artery. For both proximal and distal midgut segments, 200μm vibratome sections were prepared in ventral to dorsal direction and individually cultured in collagen gel in the absence or presence of GDNF, EDN3 or NGF. E10.5 midgut tissues that were larger or smaller than 1200±200μm, and E11.5 gut tissues with proximal midgut segments larger or smaller than 1800±200μm, were considered as over-or underdeveloped and excluded from further analysis. See Supplemental Methods section for details.

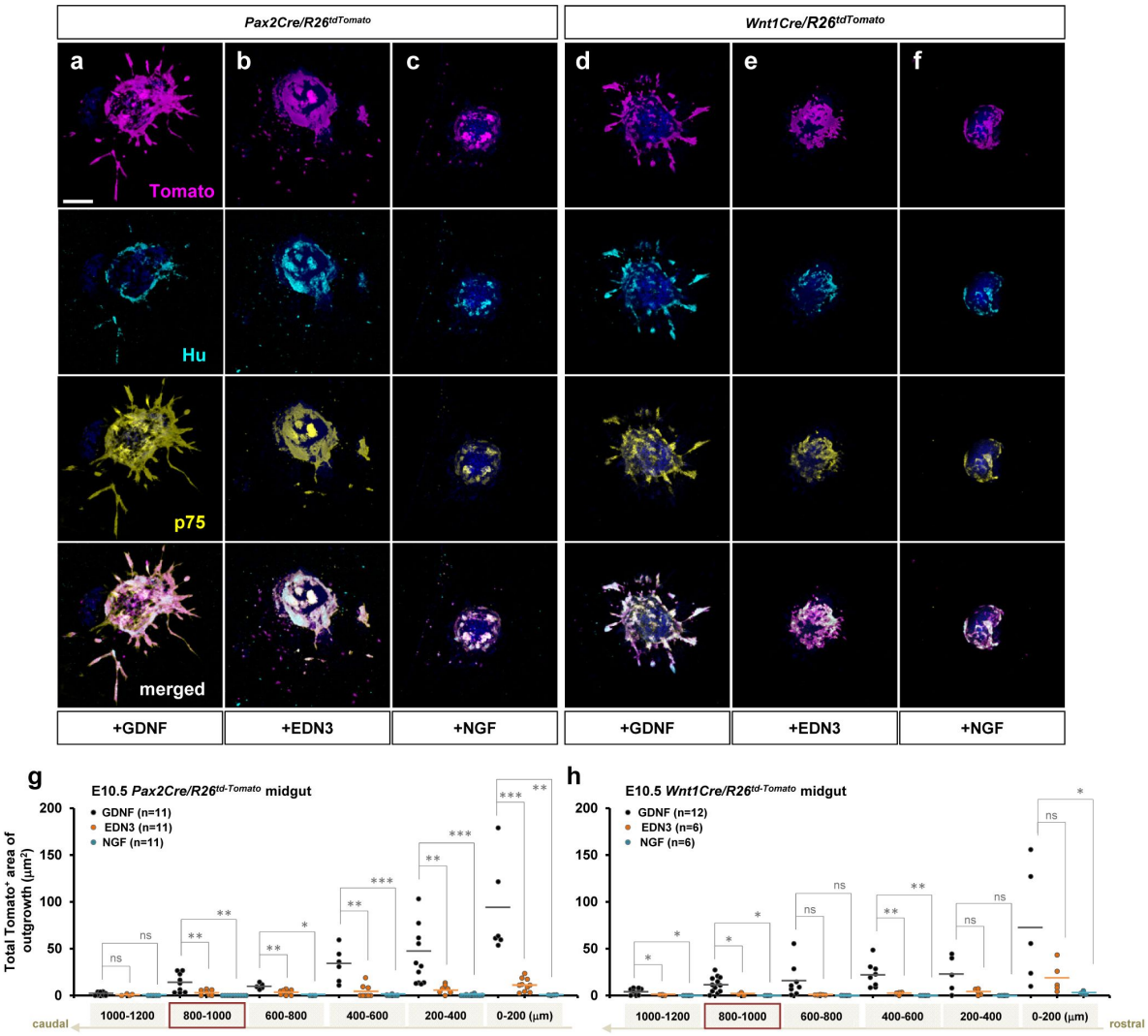

Figure 5 – figure supplement 2.

EDN3 exhibited marginal effects on E10.5 enteric progenitor outgrowth in vitro.

(a-f) Confocal z-stack images of 200µm midgut sections isolated from E10.5 *Pax2Cre/R26*$^{td\text{-}Tomato}$ (a-c) and *Wnt1Cre/R26*$^{td\text{-}Tomato}$embryos cultured for 3 days in the presence of GDNF (a), EDN3 (b) or NGF (c) and stained for neuronal Hu (cyan) and ENS progenitor marker p75 (yellow). Scale bar, 250µm. (g,h) Compiled representations of the total area of outgrowth (Tomato^{+} area around the explanted gut tube) from *Pax2Cre/R26*$^{td\text{-}Tomato}$ and *Wnt1Cre/R26*$^{td\text{-}Tomato}$ midgut slice explants in the presence of GDNF (black), EDN3 (orange), or NGF (blue). The data from GDNF treated groups here are shown as the controls in **Figure 5**. See **Figure 5** – figure supplement 1a for rostrocaudal orientation of these midgut slice preparations. Each dot represents one gut slice isolated from the indicated axial level; lost sections were not included as data points. The images shown in a-f represent sections that are 800-1000µm caudal to the foregut-midgut junction (red boxes in g and h). P-values: *$p<0.05$, **$p<0.01$, ***$p<0.001$, ns=not significant.

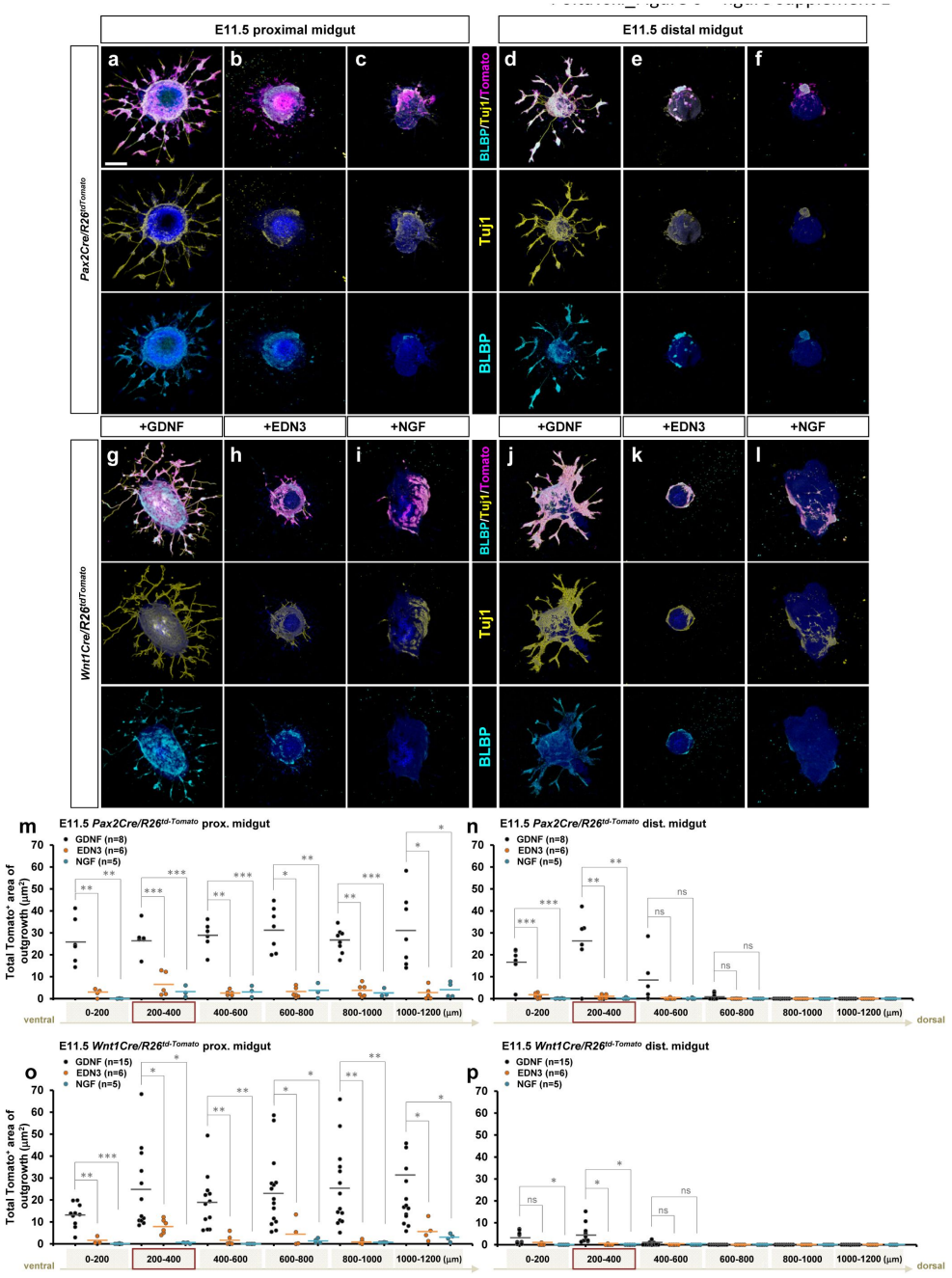

Figure 6 – figure supplement 1.

EDN3 exhibits minimal effect on E11.5 enteric progenitor outgrowth *in vitro*.

(a-h) Confocal z-stack images of 200µm proximal (a-c, g-i) and distal midgut (d-f, j-l) sections isolated from E11.5 *Pax2Cre/R26*$^{td\text{-}Tomato}$(a-f), *Wnt1Cre/R26*^{tdTomato} (g-l) embryos cultured for 3 days in the presence of GDNF (a, d, g, j), EDN3 (b, e, h, k) or NGF (c, f, I, l), and then stained for neuronal Tuj1 (yellow) and glial BLBP (cyan). Scale bars, 250µm (a-f). (m-p) Compiled representations of the total area of outgrowth in the presence of GDNF, EDN3, vs. NGF from proximal (m, o) and distal (n, p) midgut slice explants prepared from E11.5 *Pax2Cre/R26*$^{td\text{-}Tomato}$(m-n) and *Wnt1Cre/R26*^{tdTomato}(o-p) embryos. The data from GDNF treated groups here are shown as the controls in **Figure 6**. See **Figure 5** – figure supplement 1b for rostrocaudal orientation of the midgut slice preparation. The proximal midgut images shown in a-c and g-i represent sections that are 200-400 µm rostral to the apex of the midgut loop, the distal midgut images shown in d-f and j-l represent sections that are 200-400 µm caudal to the apex of the midgut loop (red boxes in m-p). P-values: *$p<0.05$, **$p<0.01$, ***$p<0.001$, ns=not significant.

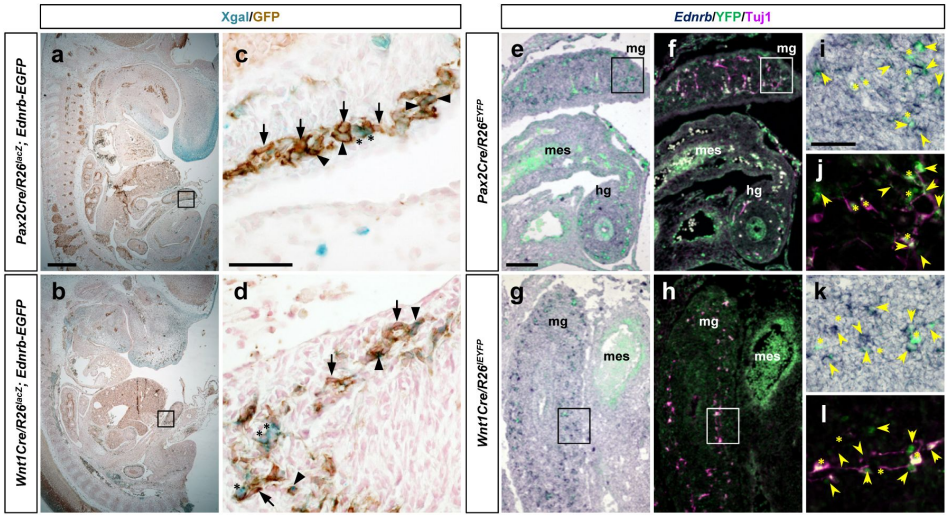

Figure 7 – figure supplement 1.

Ednrb is expressed in subsets of Pax2Cre– and Wnt1Cre-derived enteric progenitor cells.

(a-d) Histological sections of Xgal stained E12.5 *Pax2Cre/R26^{lacZ}; Ednrb-EGFP* (a) and *Wnt1Cre/R26^{lacZ}; Ednrb-EGFP* embryos immunolabeled for GFP. Magnified views of braketed areas in a and b are shown in c and d, respectively. Arrowheads point to Xgal^{+}/GFP^{+} cells, asterisks denote Xgal^{+}/GFP^{-} cells, and arrows point to Xgal^{-}/GFP^{+} cells in c and d. (e-h) Cryosections of E12.5 *Pax2Cre/R26^{EYFP}* (e-f) and *Wnt1Cre/R26^{EYFP}* (g-h) embryos at the midgut-hindgut area labeled by *in situ* hybridization for *Ednrb* gene (purple), and immunolabeled for GFP (green) and Tuj1 (magenta). Brightfield images of *Ednrb* transcripts overlaid with lineage marker YFP are shown in e and g, and their fluorescence images of YFP and Tuj1 reactive signals are shown in f and h. Magnified views of bracketed areas in e,g are shown in I,k, and in f,h in j,l. mes, mesentery. Arrows denote YFP^{+}/*Ednrb*$^{+}$ cells, asterisks indicate YFP^{+}/*Ednrb*$^{-}$ cells, and arrowheads point to YFP^{-}/*Ednrb*$^{+}$ ENS cells. Scale bars, 250μm (a-b), 50μm (c-d, i-l), 100μm (e-h).

References

1. Aldinger KA, Sokoloff G, Rosenberg DM, Palmer AA, Millen KJ (2009) **Genetic variation and population substructure in outbred CD-1 mice: implications for genome-wide association studies** *PLoS One* **4**

2. Baker CV, Bronner-Fraser M (2001) **Vertebrate cranial placodes I. Embryonic induction** *Dev Biol* **232**:1–61

3. Barald KF, Kelley MW (2004) **From placode to polarization: new tunes in inner ear development** *Development* **131**:4119–30

4. Barlow A, de Graaff E, Pachnis V (2003) **Enteric nervous system progenitors are coordinately controlled by the G protein-coupled receptor EDNRB and the receptor tyrosine kinase RET** *Neuron* **40**:905–16

5. Baynash AG, Hosoda K, Giaid A, Richardson JA, Emoto N, Hammer RE, Yanagisawa M (1994) **Interaction of endothelin-3 with endothelin-B receptor is essential for development of epidermal melanocytes and enteric neurons** *Cell* **79**:1277–85

6. Cantrell VA, Owens SE, Chandler RL, Airey DC, Bradley KM, Smith JR, Southard-Smith EM (2004) **Interactions between Sox10 and EdnrB modulate penetrance and severity of aganglionosis in the Sox10Dom mouse model of Hirschsprung disease** *Hum Mol Genet* **13**:2289–301

7. Carrasquillo MM, McCallion AS, Puffenberger EG, Kashuk CS, Nouri N, Chakravarti A (2002) **Genome-wide association study and mouse model identify interaction between RET and EDNRB pathways in Hirschsprung disease** *Nat Genet* **32**:237–44

8. Chen MK, Hsu JL, Hung MC (2020) **Nuclear receptor tyrosine kinase transport and functions in cancer** *Adv Cancer Res* **147**:59–107

9. Chen MK, Hung MC (2015) **Proteolytic cleavage, trafficking, and functions of nuclear receptor tyrosine kinases** *FEBS J* **282**:3693–721

10. Costa M, Furness JB, Pompolo S, Brookes SJ, Bornstein JC, Bredt DS, Snyder SH (1992) **Projections and chemical coding of neurons with immunoreactivity for nitric oxide synthase in the guinea-pig small intestine** *Neurosci Lett* **148**:121–5

11. D'Amico-Martel A, Noden DM (1983) **Contributions of placodal and neural crest cells to avian cranial peripheral ganglia** *Am J Anat* **166**:445–68

12. Dang R, Torigoe D, Suzuki S, Kikkawa Y, Moritoh K, Sasaki N, Agui T (2011) **Genetic background strongly modifies the severity of symptoms of Hirschsprung disease, but not hearing loss in rats carrying Ednrb(sl) mutations** *PLoS One* **6**

13. Danielian PS, Muccino D, Rowitch DH, Michael SK, McMahon AP (1998) **Modification of gene activity in mouse embryos in utero by a tamoxifen-inducible form of Cre recombinase** *Curr Biol* **8**:1323–6

14. Durbec PL, Larsson-Blomberg LB, Schuchardt A, Costantini F, Pachnis V (1996) **Common origin and developmental dependence on c-ret of subsets of enteric and sympathetic neuroblasts** *Development* **122**:349–58

15. Fuchs S, Amiel J, Claudel S, Lyonnet S, Corvol P, Pinet F (2001) **Functional characterization of three mutations of the endothelin B receptor gene in patients with Hirschsprung's disease: evidence for selective loss of Gi coupling** *Mol Med* **7**:115–24

16. Furness J (2006) **The Enteric Nervous System** Blackwell

17. Gong S, Doughty M, Harbaugh CR, Cummins A, Hatten ME, Heintz N, Gerfen CR (2007) **Targeting Cre recombinase to specific neuron populations with bacterial artificial chromosome constructs** *J Neurosci* **27**:9817–23

18. Goto A, Sumiyama K, Kamioka Y, Nakasyo E, Ito K, Iwasaki M, Enomoto H, Matsuda M (2013) **GDNF and endothelin 3 regulate migration of enteric neural crest-derived cells via protein kinase A and Rac1** *J Neurosci* **33**:4901–12

19. Grantcharova E, Reusch HP, Grossmann S, Eichhorst J, Krell HW, Beyermann M, Rosenthal W, Oksche A (2006) **N-terminal proteolysis of the endothelin B receptor abolishes its ability to induce EGF receptor transactivation and contractile protein expression in vascular smooth muscle cells** *Arterioscler Thromb Vasc Biol* **26**:1288–96

20. Guthrie S, Lumsden A (1994) **Collagen Gel Coculture of Neural Tissue** *Neuroprotocols* **4**:116–120

21. Harun-Or-Rashid M, Konjusha D, Galindo-Romero C, Hallbook F (2016) **Endothelin B Receptors on Primary Chicken Muller Cells and the Human MIO-M1 Muller Cell Line Activate ERK Signaling via Transactivation of Epidermal Growth Factor Receptors** *PLoS One* **11**

22. Hosoda K, Hammer RE, Richardson JA, Baynash AG, Cheung JC, Giaid A, Yanagisawa M (1994) **Targeted and natural (piebald-lethal) mutations of endothelin-B receptor gene produce megacolon associated with spotted coat color in mice** *Cell* **79**:1267–76

23. Kapur RP (2000) **Colonization of the murine hindgut by sacral crest-derived neural precursors: experimental support for an evolutionarily conserved model** *Dev Biol* **227**:146–55

24. Keast JR (1995) **Visualization and immunohistochemical characterization of sympathetic and parasympathetic neurons in the male rat major pelvic ganglion** *Neuroscience* **66**:655–62

25. Kilpatrick LE, Hill SJ (2021) **Transactivation of G protein-coupled receptors (GPCRs) and receptor tyrosine kinases (RTKs): Recent insights using luminescence and fluorescence technologies** *Curr Opin Endocr Metab Res* **16**:102–112

26. Kuruvilla R, Zweifel LS, Glebova NO, Lonze BE, Valdez G, Ye H, Ginty DD (2004) **A neurotrophin signaling cascade coordinates sympathetic neuron development through differential control of TrkA trafficking and retrograde signaling** *Cell* **118**:243–55

27. Ladher RK, O'Neill P, Begbie J (2010) **From shared lineage to distinct functions: the development of the inner ear and epibranchial placodes** *Development* **137**:1777–85

28. Lake JI, Heuckeroth RO (2013) **Enteric nervous system development: migration, differentiation, and disease** *Am J Physiol Gastrointest Liver Physiol* **305**:G1–24

29. Le Douarin NM (1982) **The Neural Crest** Cambridge University Press

30. Luo W, Wickramasinghe SR, Savitt JM, Griffin JW, Dawson TM, Ginty DD (2007) **A hierarchical NGF signaling cascade controls Ret-dependent and Ret-independent events during development of nonpeptidergic DRG neurons** *Neuron* **54**:739–54

31. Madisen L *et al.* (2010) **A robust and high-throughput Cre reporting and characterization system for the whole mouse brain** *Nat Neurosci* **13**:133–40

32. Mahato AK, Sidorova YA (2020) **RET Receptor Tyrosine Kinase: Role in Neurodegeneration, Obesity, and Cancer** *Int J Mol Sci* **21**

33. Makita T, Sucov HM, Gariepy CE, Yanagisawa M, Ginty DD (2008) **Endothelins are vascular-derived axonal guidance cues for developing sympathetic neurons** *Nature* **452**:759–63

34. McCallion AS, Stames E, Conlon RA, Chakravarti A (2003) **Phenotype variation in two-locus mouse models of Hirschsprung disease: tissue-specific interaction between Ret and Ednrb** *Proc Natl Acad Sci U S A* **100**:1826–31

35. Mitchell PJ, Timmons PM, Hebert JM, Rigby PW, Tjian R (1991) **Transcription factor AP-2 is expressed in neural crest cell lineages during mouse embryogenesis** *Genes Dev* **5**:105–19

36. Mueller JL, Goldstein AM (2022) **The science of Hirschsprung disease: What we know and where we are headed** *Semin Pediatr Surg* **31**

37. Nagy N, Goldstein AM (2017) **Enteric nervous system development: A crest cell's journey from neural tube to colon** *Semin Cell Dev Biol* **66**:94–106

38. Ohyama T, Groves AK (2004) **Generation of Pax2-Cre mice by modification of a Pax2 bacterial artificial chromosome** *Genesis* **38**:195–9

39. Parisi MA, Kapur RP (2000) **Genetics of Hirschsprung disease** *Curr Opin Pediatr* **12**:610–7

40. Prigge JR, Wiley JA, Talago EA, Young EM, Johns LL, Kundert JA, Sonsteng KM, Halford WP, Capecchi MR, Schmidt EE (2013) **Nuclear double-fluorescent reporter for in vivo and ex vivo analyses of biological transitions in mouse nuclei** *Mamm Genome* **24**:389–399

41. Rattner A, Yu H, Williams J, Smallwood PM, Nathans J (2013) **Endothelin-2 signaling in the neural retina promotes the endothelial tip cell state and inhibits angiogenesis** *Proc Natl Acad Sci U S A* **110**:E3830–9

42. Sanchez MP, Silos-Santiago I, Frisen J, He B, Lira SA, Barbacid M (1996) **Renal agenesis and the absence of enteric neurons in mice lacking GDNF** *Nature* **382**:70–3

43. Sang Q, Young HM (1996) **Chemical coding of neurons in the myenteric plexus and external muscle of the small and large intestine of the mouse** *Cell Tissue Res* **284**:39–53

44. Sarna SK (2010) **Colonic Motility: From Bench Side to Bedside** Morgan & Claypool Life Sciences

45. Schuchardt A, D'Agati V, Larsson-Blomberg L, Costantini F, Pachnis V (1994) **Defects in the kidney and enteric nervous system of mice lacking the tyrosine kinase receptor Ret** *Nature* **367**:380–3

46. Serbedzija GN, Bronner-Fraser M, Fraser SE (1989) **A vital dye analysis of the timing and pathways of avian trunk neural crest cell migration** *Development* **106**:809–16

47. Soriano P (1999) **Generalized lacZ expression with the ROSA26 Cre reporter strain** *Nat Genet* **21**:70–1

48. Southard-Smith EM, Kos L, Pavan WJ (1998) **Sox10 mutation disrupts neural crest development in Dom Hirschsprung mouse model** *Nat Genet* **18**:60–4

49. Srinivas S, Watanabe T, Lin CS, William CM, Tanabe Y, Jessell TM, Costantini F (2001) **Cre reporter strains produced by targeted insertion of EYFP and ECFP into the ROSA26 locus** *BMC Dev Biol* **1**

50. Tan JVS, Duron A, Sucov HM, Makita T (2023) **Placode and neural crest origins of congenital deafness in mouse models of Waardenburg-Shah syndrome** *bioRxiv*

51. Theveneau E, Mayor R (2012) **Neural crest delamination and migration: from epithelium-to-mesenchyme transition to collective cell migration** *Dev Biol* **366**:34–54

52. Timmermans JP, Barbiers M, Scheuermann DW, Bogers JJ, Adriaensen D, Fekete E, Mayer B, Van Marck EA, De Groodt-Lasseel MH (1994) **Nitric oxide synthase immunoreactivity in the enteric nervous system of the developing human digestive tract** *Cell Tissue Res* **275**:235–45

53. Tsuchioka M, Takebayashi M, Hisaoka K, Maeda N, Nakata Y (2008) **Serotonin (5-HT) induces glial cell line-derived neurotrophic factor (GDNF) mRNA expression via the transactivation of fibroblast growth factor receptor 2 (FGFR2) in rat C6 glioma cells** *J Neurochem* **106**:244–57

54. Uesaka T, Nagashimada M, Enomoto H (2015) **Neuronal Differentiation in Schwann Cell Lineage Underlies Postnatal Neurogenesis in the Enteric Nervous System** *J Neurosci* **35**:9879–88

55. Wolfson RL, Abdelaziz A, Rankin G, Kushner S, Qi L, Mazor O, Choi S, Sharma N, Ginty DD (2023) **DRG afferents that mediate physiologic and pathologic mechanosensation from the distal colon** *Cell* **186**:3368–3385

56. Yamauchi Y, Abe K, Mantani A, Hitoshi Y, Suzuki M, Osuzu F, Kuratani S, Yamamura K (1999) **A novel transgenic technique that allows specific marking of the neural crest cell lineage in mice** *Dev Biol* **212**:191–203

57. Yu Q *et al.* (2024) **Sacral Neural Crest-Independent Origin of the Enteric Nervous System in Mouse** *Gastroenterology* **166**:1085–1099

Author information

Denise M Poltavski*
Department of Regenerative Medicine and Cell Biology, Medical University of South Carolina, Charleston, USA

*These authors contribute equally to this work

Alexander T Cunha*
Department of Regenerative Medicine and Cell Biology, Medical University of South Carolina, Charleston, USA

*These authors contribute equally to this work

Jaime Tan
Department of Regenerative Medicine and Cell Biology, Medical University of South Carolina, Charleston, USA

Henry M Sucov
Department of Regenerative Medicine and Cell Biology, Medical University of South Carolina, Charleston, USA

Takako Makita
Department of Regenerative Medicine and Cell Biology, Medical University of South Carolina, Charleston, USA
ORCID iD: 0000-0002-5598-5690

For correspondence: makita@musc.edu

Editors

Reviewing Editor
Samuel Pleasure
University of California, San Francisco, San Francisco, United States of America

Senior Editor
Didier Stainier
Max Planck Institute for Heart and Lung Research, Bad Nauheim, Germany

Reviewer #1 (Public Review):

Summary:

The manuscript by Poltavski and colleagues describes the discovery of previously unreported enteric neural crest-derived cells (ENCDC) which are marked by Pax2 and originating from the Placodes. By creating multiple conditional mouse mutants, the authors demonstrate these cells are a distinct population from the previously reported ENCDCs which originate from the Vagal neural crest cells and express Wnt1.

These Pax2-positive ENCDCs are affected due to the loss of both Ret and Ednrb highlighting that these cells are also ultimately part of the canonical processes governing ENCDC and enteric nervous system (ENS) development. The authors also make explant cultures from the mouse GI tract to detect how Ednrb signaling is important for Ret signaling pathways in these

cells and rediscovers the interactions between these 2 pathways. One important observation the authors make is that CGRP-positive neurons in the adult distal colon seem to be primarily derived from these Pax2-positive ENCDCs, which are significantly reduced in the Ednrb mutants, thus highlighting the role of Ednrb in maintaining this neuronal type.

Comments on latest version:

Author response: We disagree that the datasets from previous studies provide additional insights that are relevant to the current study. It must be appreciated that Wnt1Cre and Pax2Cre are genetic lineage tracers and that migratory ENS progenitor cells labeled with these reagents do not maintain expression of Wnt1 and Pax2 mRNA or protein. The Wnt1 and Pax2 genes are only transiently expressed within their distinct regions of the ectoderm, and their expression turns off as cells delaminate and begin migration. Thus, Pax2Cre-labeled ENS progenitor cells are not Pax2-positive thereafter. The single cell RNA-Seq studies suggested by the reviewer were collected from older embryos and postnatal mice, and do not represent the E10.5-E11.5 period that accounts for genesis of Ret-mediated and Ednrb-mediated Hirschsprung disease pathology. Even with the most recent work by Zhou et al (Dev Cell, 2024) that included E10.5 cells, this analysis only evaluated neural crest-derived Sox10Cre lineage cells, which does not include the placode-derived Pax2Cre lineage (as we show explicitly in Fig. 2-figure supplement 2). Consequently, it would not be possible to find the "Pax2-positive cells" in these datasets. Performing a new transcriptomic analysis by isolating Pax2Cre-lineage and Wnt1Cre-lineage cells at the appropriate developmental time points could be the basis of future studies, but we think these are beyond the scope of the present paper.

Reviewer comment: Since these cells are a completely new discovery, additional validation would be beneficial. Whole early GI tract datasets are available, such as human 6-week fetal gut data (PMID: 29802404) and whole mouse embryo studies spanning development that include ENS (PMID: 38355799). If the authors believe that none of these existing datasets can detect these cells in their developmental state and that targeted cell studies with specific Cre drivers would be required, they should make this explicitly clear.

A key advantage of discovering a new cell type, particularly in the relatively understudied field of ENS, is the opportunity for the broader community to leverage this finding to inform their own research. If these cells are absent from current datasets, even those covering the whole GI tract, this should be clearly communicated.

I aim to support the authors here. New discoveries in science require robust validation to enhance their impact. The authors have generated an important reagent with great potential for broader use, and addressing these straightforward requests would strengthen the study and make it more valuable to the scientific community.

Author response: The observation that human mutations in RET and EDNRB both cause Hirschsprung disease is decades old, and of course numerous studies in human, mouse, and cells have addressed the relation between the two signaling pathways. We did not mean to imply that we were the first to discover that Ret and Ednrb signaling pathways interact. The reviewer cites a number of papers all from the Chakravarti lab that address this phenomenon; while these are a valuable contribution to the field, there is still more to be learned. The model elaborated in PMID: 31313802, in which Ret and Ednrb are both enmeshed in a common gene regulatory network, does not readily explain why each has a different phenotypic manifestation and doesn't take into account the importance of the placodal lineage. The main new contributions of our paper are the existence of a new cell lineage that contributes to the ENS, and that the placodal and neural crest lineages utilize Ret and Ednrb signaling differently. The clarification of how these elements are differentially used by the two lineages explains long-segment and short-segment Hirschsprung disease (Ret and Ednrb mutants, respectively) far better than in past studies. The reviewer unfortunately

dismisses these insights and seems to feel that a biochemical exploration of one specific component of the signaling interaction (Y1015 phosphorylation) would be more relevant. This should be the basis of future studies and are beyond the scope of the new findings reported in the present paper

Reviewer comment: The authors completely miss the point. There is no association between phenotypic severity (L-HSCR, S-HSCR, or TCA) and mutations in a given gene in HSCR. EDNRB, for example, has a syndromic association with Waardenburg-Shah syndrome (WS4-A), which includes pigmentation anomalies due to EDNRB expression in neural crest cells that give rise to pigment cells.

The authors' discovery reinforces the current paradigm that nearly all HSCR is mediated by mutations in genes within the GRN, accounting for 72% of the population attributable risk. This is valuable; reinforcing established paradigms with new data is crucial, and the authors should appreciate the significance of this contribution.

The discovery of the signaling interaction is particularly important, as it offers a potential explanation for disease severity and provides a basis for classifying patients in future sequencing studies. It is surprising that the authors seem reluctant to highlight this novel finding, as it could greatly benefit future research, including the development of specific mouse mutants and advancing human genetics studies.

Author response: The reviewer overlooked that one of the review articles that we cited (Chen, Hsu, & Hung, 2020) has a dedicated paragraph for RET (section 3.14), which summarizes the work by Barheri-Yarmand et al (PMID: 25795775) which is the very paper noted by the reviewer in the comment above. The reviewer also somewhat misstated the results of the Barheri-Yarmand et al study. By immunostaining, this paper showed nuclear localization of endogenous Ret, albeit a version of Ret with a disease-associated mutation that makes it constitutively active by constitutive autophosphorylation. Nonetheless, this was endogenous Ret. The paper also used overexpression of GFP-tagged RET in HEK293 cells to show that wildtype RET can behave in a similar manner, at least under these circumstances. Our point is simply that Ret (and other receptor tyrosine kinases) can be found in the nucleus in certain biological contexts, and our observations are consistent with this precedent. The reviewer also suggests a biochemical follow-up analysis related to this observation, which we agree would be of interest. Such an investigation however is beyond the scope of the present study.

Reviewer comment: As the authors themselves now highlight from the cited paper that any evidence of RET entering the nucleus is of a mutant RET protein, How does this align with their discovery for wildtype protein?

This finding of nuclear localization of RET is both intriguing and unprecedented. Despite extensive biochemical studies on RET, given its role as an oncogene, this feature has not been identified before. If validated, this discovery could significantly advance the field and improve interpretation of future studies. I reiterate my previous point: a novel finding that challenges the current paradigm requires additional evidence.

https://doi.org/10.7554/eLife.96424.2.sa2

Reviewer #2 (Public review):

Summary:

This manuscript by Poltavski and colleagues explores the relative contributions of Pax2- and Wnt1- lineage derived cells in the enteric nervous system (ENS) and how they are each affected by disruptions in Ret and Endrb signaling. The current understanding of ENS development in mice is that vagal neural crest progenitors derived from a Wnt1+ lineage

migrate into and colonize the developing gut. The sacral neural crest was thought to make a small contribution to the hindgut in addition but recent work has questioned that contribution and shown that the ENS is entirely populated by vagal crest (PMID: 38452824). GDNF-Ret and Endothelin3-Ednrb signaling are both known to be essential for normal ENS development and loss of function mutations are associated with a congenital disorder called Hirschsprung's disease. The transcription factor Pax2 has been studied in CNS and cranial placode development but has not been previously implicated in ENS development. In this work, the authors begin with the unexpected observation that conditional knockout of Ednrb in Pax2-expressing cells causes a similar aganglionosis, growth retardation, and obstructed defecation as conditional knockout of Ednrb in Wnt1-expressing cells. The investigators then use the Pax2 and Wnt1 Cre transgenic lines to lineage-trace ENS derivatives and assess the effects of loss of Ret or Ednrb during embryonic development in these lineages. Finally, they use explants from the corresponding embryos to examine the effects of GDNF on progenitor outgrowth and differentiation.

Strengths:

- The manuscript is overall very well illustrated with high resolution images and figures. Extensive data are presented.

- The identification of Pax2 expression as a lineage marker that distinguishes a subset of cells in the ENS that may be distinct from cells derived from Wnt1+ progenitors is an interesting new observation that challenges current understanding of ENS development

- Pax2 has not been previously implicated in ENS development - this manuscript does not directly test that role but hints at the possibility

- Interrogation of two distinct signaling pathways involved in ENS development and their relative effects on the two purported lineages

Weaknesses:

- The major challenge with interpreting this work is the use of two transgenic lines, Wnt1-Cre and Pax2-Cre, which are not well characterized in terms of fidelity to native gene expression and recombination efficiency in the ENS. If 100% of cells that express Wnt1 do not express Cre or if the Pax2 transgene is expressed in cells that do not normally express Pax2, then these observations would have very different interpretations and would not support the conclusions made. The two lineages are never compared in the same embryo, which also makes it difficult to assess relative contributions and renders the evidence more circumstantial than definitive.

- Visualization of the Pax2-Cre and Wnt-1Cre induced recombination in cross-sections at postnatal ages would help with data interpretation. If there is recombination evident in the mesenchyme, this would particularly alter interpretation of Ednrb mutant experiments, since that pathway has been shown to alter gut mesenchyme and ECM, which could indirectly alter ENS colonization.

- The data on distinct lineages in Fig 3 is somewhat weak and the description in the Results section tends to over-interpretation. For example, "A minimum number (approx. 3%) of CGRP+ neurons were labeled by Wnt1Cre ... which indicates that Wnt1Cre-derived cells have little or no commitment to a mechanosensory fate in the distal colon." The data panel in Fig 3f shows that most of the CGRP-IR cells in Wnt1-Cre-Tomato mice are tdTomato+ though their tdTomato fluorescence is less intense than in neighboring smaller, likely glial cells. This suggests that CGRP+/Tomato+ neurons were likely undercounted. IHC for tdTomato to ensure detection of low levels of Tomato expression and quantification of observations would strengthen the authors' claim. CGRP+ enteric neurons have been visualized and functionally described by several investigators in the field using Wnt1-Cre-GCaMP mice, which also

challenges the authors' conclusions. Finally, quantification of CGRP+ enteric neurons by measuring CGRP mucosal fiber immunoreactivity is not accurate because it would reflect both ENS CGRP-expressing neurons and visceral afferents from DRG. Moreover, it is not known if all CGRP+ enteric neurons project to the mucosa or if all mucosal-projecting neurons are mechanosensory. Finally, most of the signal seems to be non-specific background staining in the mucosa and quantification of mucosal signal in this context does not seem meaningful.

- No consideration of glia - are these derived from both lineages?

- No discussion of how these observations may fit in with recent work that suggests a mesenchymal contribution of enteric neurons (PMID: 38108810)

- Phospho-RET staining in Figure 7 is difficult to discern and interpret with high background. Positive and negative controls would strengthen these data.

Comments on revised version:

The authors have responded to the weaknesses identified above. Based on my own assessment of the revised manuscript, my assessment is unchanged because the manuscript is largely unchanged.

https://doi.org/10.7554/eLife.96424.2.sa1

Author response:

The following is the authors' response to the original reviews.

> ***Reviewer #1 (Public Review):***
>
> *The manuscript by Poltavski and colleagues describes the discovery of previously unreported enteric neural crestderived cells (ENCDC) which are marked by Pax2 and originating from the Placodes. By creating multiple conditional mouse mutants, the authors demonstrate these cells are a distinct population from the previously reported ENCDCs which originate from the Vagal neural crest cells and express Wnt1.*
>
> *These Pax2-positive ENCDCs are affected due to the loss of both Ret and Ednrb highlighting that these cells are also ultimately part of the canonical processes governing ENCDC and enteric nervous system (ENS) development. The authors also make explant cultures from the mouse GI tract to detect how Ednrb signaling is important for Ret signaling pathways in these cells and rediscovers the interactions between these 2 pathways. One important observation the authors make is that CGRP-positive neurons in the adult distal colon seem to be primarily derived from these Pax2-positive ENCDCs, which are significantly reduced in the Ednrb mutants, thus highlighting the role of Ednrb in maintaining this neuronal type.*
>
> *I appreciate the amount of work the authors have put into generating the mouse models to detect these cells, but there isn't any new insight on either the nature of ENCDC development or the role of Ret and Ednrb. Also, there are sophisticated single-cell genomics methods to detect rare cell type/states these days and the authors should either employ some of those themselves in these mouse models or look at extensively publicly available single-cell datasets of the developing wildtype and mutant mouse and human ENS to map out the global transcriptional profile of these cells. A more detailed analysis of these Pax2-positive cells would be really helpful to both the ENS community as well as researchers studying gut motility disorders.*

We would like to point out that the reviewer's comments in both Public Review and in some cases reiterated in Recommendations for the Authors are rooted in several misunderstandings. The reviewer writes "Pax2-positive ENCDCs", as if the Pax2 lineage (properly, the Pax2Cre-labeled lineage) of the ENS is a subset of neural crest, and states that "there isn't any new insight" from our study on ENS development. Our conclusion is quite different, that the Pax2Cre lineage (placode-derived) is distinct from the neural crest-derived cell lineage. The reviewer may not have appreciated that our study establishes a fundamental reinterpretation of the very long-standing dogma that the ENS is derived solely from neural crest. We believe that finding and characterizing the unique contribution of an independent cell lineage to the ENS provides critical new perspectives into ENS development and the etiology of Hirschsprung disease. One feature of the Pax2Cre (placodal) lineage is as the source of CGRP-positive mechanosensory neurons in the colon (as the reviewer mentioned), but this is one feature of the larger conceptual discovery of the existence of a separate lineage contribution to the ENS, not the most important observation in and of itself.

The reviewer continues by saying that we "rediscovered" the interaction between Ednrb and Ret in ENS development. In our study we show that the two lineages (placode-derived and neural crest-derived) employ Ednrb and Ret signaling in distinct ways. This isn't simply rediscovery, this is new insight. To the extent that both lineages utilize both signaling axes (albeit with mechanistic differences) is a primary reason why the unique placodal lineage contribution to the ENS remained unsuspected until now. We have revised the text to make these points more clear in our revised manuscript.

The reviewer also suggests single cell genomic methods, which is addressed below in our response to the reviewer's first recommendation.

> ***Reviewer #2 (Public Review):***
>
> *This manuscript by Poltavski and colleagues explores the relative contributions of Pax2- and Wnt1- lineagederived cells in the enteric nervous system (ENS) and how they are each affected by disruptions in Ret and Endrb signaling. The current understanding of ENS development in mice is that vagal neural crest progenitors derived from a Wnt1+ lineage migrate into and colonize the developing gut. The sacral neural crest was thought to make a small contribution to the hindgut in addition but recent work has questioned that contribution and shown that the ENS is entirely populated by the vagal crest (PMID: 38452824). GDNF-Ret and Endothelin3-Ednrb signaling are both known to be essential for normal ENS development and loss of function mutations are associated with a congenital disorder called Hirschsprung's disease. The transcription factor Pax2 has been studied in CNS and cranial placode development but has not been previously implicated in ENS development. In this work, the authors begin with the unexpected observation that conditional knockout of Ednrb in Pax2-expressing cells causes a similar aganglionosis, growth retardation, and obstructed defecation as conditional knockout of Ednrb in Wnt1-expressing cells. The investigators then use the Pax2 and Wnt1 Cre transgenic lines to lineage-trace ENS derivatives and assess the effects of loss of Ret or Ednrb during embryonic development in these lineages. Finally, they use explants from the corresponding embryos to examine the effects of GDNF on progenitor outgrowth and differentiation.*
>
> *Strengths:*
>
> *- The manuscript is overall very well illustrated with high-resolution images and figures. Extensive data are presented.*
>
> *- The identification of Pax2 expression as a lineage marker that distinguishes a subset of cells in the ENS that may be distinct from cells derived from Wnt1+ progenitors is an*

> *interesting new observation that challenges the current understanding of ENS development.*
>
> *- Pax2 has not been previously implicated in ENS development - this manuscript does not directly test that role but hints at the possibility.*
>
> *- Interrogation of two distinct signaling pathways involved in ENS development and their relative effects on the two purported lineages.*

The reviewer provided a succinct and accurate summary of our analysis. We correct just the one statement that the ENS is entirely populated by vagal crest. The paper cited by the reviewer (PMID: 38452824) used Wnt1DreERT2 to lineage label the NC population, so of course only looked at neural crest (comparing vagal vs. sacral NC). The advance in our study is to newly document the independent contribution of the placodal lineage.

> *Weaknesses:*
>
> *- The major challenge with interpreting this work is the use of two transgenic lines, rather than knock-ins, Wnt1Cre and Pax2-Cre, which are not well characterized in terms of fidelity to native gene expression and recombination efficiency in the ENS. If 100% of cells that express Wnt1 do not express this transgene or if the Pax2 transgene is expressed in cells that do not normally express Pax2, then these observations would have very different interpretations and not support the conclusions made. The two lineages are never compared in the same embryo, which also makes it difficult to assess relative contributions and renders the evidence more circumstantial than definitive.*

We do not agree that the Cre lines being transgenics rather than knock-ins changes the utility of these reagents or the interpretation of the results; there are also potential problems with knock-in alleles. Wnt1Cre has been in use for 25 years as a pan-neural crest lineage cell marker with exceptional efficiency and specificity (including numerous studies of the ENS), so we disagree that it is not well characterized. Pax2Cre of course has not previously been studied in the ENS, but it has been broadly used in other contexts (e.g., craniofacial, kidney). That said, and as noted in our original manuscript, we are aware that an issue of this study is the uniqueness of the recombination domains of the two Cre lines. As we wrote, Wnt1Cre and Pax2Cre cannot be combined into the same embryo because they are both Cre lines, and we do not have a suitable nonCre recombinase line to substitute for either. Instead, we demonstrate that the two lines recombine in distinct territories of the early embryonic ectoderm, and that the two lineages thus labeled are distinct in marker expression at the initial onset of their delamination, utilize Edn3-Ednrb and GDNF-Ret in distinct ways during their migration to the hindgut, and contribute to different terminal cell fates in the colon. We think this evidence of the distinct nature of the two lineages from start to finish is compelling rather than merely circumstantial.

> *- Visualization of the Pax2-Cre and Wnt-1Cre induced recombination in cross-sections at postnatal ages would help with data interpretation. If there is recombination induced in the mesenchyme, this would particularly alter the interpretation of Ednrb mutant experiments, since that pathway has been shown to alter gut mesenchyme and ECM, which could indirectly alter ENS colonization.*

We have several thoughts about this comment. First, we are uncertain why postnatal analysis would be informative, as ENS colonization occurs (or fails to occur in mutants) during embryogenesis. The reviewer might be thinking of a juvenile stage additional contribution to the ENS, which is addressed below (responses to *Recommendations for the Authors*) but as we discuss there is not relevant to our analysis. Second, we did examine recombination in the distal hindgut at E12.5 during ENS colonization (Fig. 1f and 1h) and did not see overlap

between either Cre recombination domain and *Edn3* mRNA expression (which is expressed by the nonENS mesenchyme). Furthermore, Ednrb is not expressed in the gut mesenchyme during ENS colonization (Fig. 7figure supplement 1), thus ectopic mesenchymal Cre expression, if any, by either line would have no impact in Cre/Ednrb mutants. Lastly, the reviewer's idea could have been a plausible hypothesis at the onset of the project, but here we show positive evidence for a different explanation. We do not rigorously exclude the reviewer's hypothesis, nor other theoretically possible models, but we think we have provided a strong case to support the direct involvement of Ret and Ednrb in ENS progenitors rather than in surrounding non-neural mesenchyme.

> *- No consideration of glia - are these derived from both lineages?*

To properly address this question would require new reagents and analyses that we have not yet initiated. While an interesting question from a developmental biology standpoint, we don't think that this investigation would change any of the interpretations that we make in the manuscript.

> *- No discussion of how these observations may fit in with recent work that suggests a mesenchymal contribution of enteric neurons (PMID: 38108810).*

The recent paper cited by the reviewer is very explicit in describing this mesenchymal contribution to the ENS as occurring after postnatal day P11. Other than the terminal Hirschsprung phenotype, all of our analysis of cell lineage migration and fate and colonic aganglionosis was conducted at embryonic or early (P9) postnatal stages. We therefore do not see a relation of our work to this study. In light of this paper, however, we do agree that it would be worthwhile in a future study to explore Wnt1Cre and Pax2Cre lineage dynamics in the ENS of older mice.

> ***Reviewer #1 (Recommendations For The Authors):***
>
> *(1) The authors should reanalyze multiple single-cell RNA-seq datasets available now, to see if these cells are detected in those studies and then look at the global transcriptional profile of these Pax2-positive cells compared to the other vagal neural crest-derived ENCDCs. Some of these datasets can be found here - PMIDs: 33288908, 37585461, and https://www.gutcellatlas.org/.*

We disagree that the datasets from previous studies provide additional insights that are relevant to the current study. It must be appreciated that Wnt1Cre and Pax2Cre are genetic lineage tracers and that migratory ENS progenitor cells labeled with these reagents do not maintain expression of Wnt1 and Pax2 mRNA or protein. The *Wnt1* and *Pax2* genes are only transiently expressed within their distinct regions of the ectoderm, and their expression turns off as cells delaminate and begin migration. Thus, Pax2Cre-labeled ENS progenitor cells are not Pax2-positive thereafter. The single cell RNA-Seq studies suggested by the reviewer were collected from older embryos and postnatal mice, and do not represent the E10.5-E11.5 period that accounts for genesis of Ret-mediated and Ednrb-mediated Hirschsprung disease pathology. Even with the most recent work by Zhou et al (Dev Cell, 2024) that included E10.5 cells, this analysis only evaluated neural crest-derived Sox10Cre lineage cells, which does not include the placode-derived Pax2Cre lineage (as we show explicitly in Fig. 2-figure supplement 2). Consequently, it would not be possible to find the "Pax2-positive cells" in these datasets. Performing a new transcriptomic analysis by isolating Pax2Cre-lineage and Wnt1Cre-lineage cells at the appropriate developmental time points could be the basis of future studies, but we think these are beyond the scope of the present paper.

> *(2) Even in their current quantification method of using immunofluorescent cells in a microscopic field, the authors count very few cells. The quantification in Figures 2v-2z is only from 4 embryos and is in the hundreds. This leads to misrepresentation of cell numbers and is best reflected in Figure 2x, where Wnt1Cre/Ret GI tracts have 0 Ret +ve cells, which we now know is not true even in ubiquitous Ret null embryos, where Ret null cells are detected as late as E14.5 (PMID 37585461)*

Because of the reviewer's comment, we recognize that the specific detail about cell numbers wasn't properly written. We didn't count a few hundred cells total, it was a few hundred cells per embryo. Exact numbers are provided in the revised figure legend where "cells/embryo" is now explicitly stated. Multiplied by the number of embryos, this means that we evaluated approx. 1000 total cells per genotype and time point in cases where Ret+ and/or GFP+ (lineage+) cells were found. The total absence of such cells in Wnt1Cre/Ret mutants is a rigorous conclusion. Our results do not misrepresent nor contradict the study by Vincent et al (PMID 37585461). Our analyses were performed on gut tissue isolated at E10.5 and E11.5 stages, which is long before Schwann cell precursors (SCPs, the primary focus of the Vincent et al study) colonize the gut (E14.5; Uesaka et al, 2015. PMID: 26156989). Indeed, as the reviewer notes, SCPs migrate into the gut in a Retindependent manner. For being at a much earlier time point, our focus is on the cranial ectoderm sources of ENS progenitors. We have adjusted the text associated with Fig. 2 to make this more clear.

> *(3) There are multiple sections in the manuscript that rehash already known facts, like the whole section about Wnt1 conditional Ret null mice which show failure of migration of ENCDCs. This has been shown multiple times and doesn't add anything to the author's story.*

We think this comment stems from the reviewer's perception that the Pax2Cre lineage is a subset of neural crest. The Wnt1Cre data (including Ret-deficient and Ednrb-deficient embryos) presented in the manuscript are not intended to rehash what is already known but to establish important similarities and differences between the newly identified placode-derived and the well-established neural crest-derived ENS progenitor cells. In light of the reviewer's suggestion #8 below, to move the Wnt1Cre lineage analysis to a supplement, this information remains in the main text to provide proper comparison to the Pax2Cre-lineage profile. We think we were fair in the text to the legacy of work on neural crest and ENS development and were explicit in using our Wnt1Cre analysis to compare to the Pax2Cre lineage. Finally, we point out that our analysis was conducted on a different genetic background (outbred ICR) compared to previous studies, and there are strain-specific differences in Hirschsprung-associated lethality between our background and previous studies, so it was not impossible that the behavior of the neural crest cell lineage in the ICR background could be different from past observations on different backgrounds. Although we did not identify any major differences, it is important that the information on NC behavior in this background be presented.

> *(4) Also, the conclusion drawn for Figure 5C "this indicates that the Wnt1Cre-derived cells do not harbor a cellautonomous response to GDNF" seems to suggest the authors are not very well versed with the ENS literature. GDNF as well as EDN3 are expressed from surrounding mesenchyme and are cell non-autonomous.*

The reviewer seems to have misread or misunderstood the specific statement as well as the more important broader conclusion of the experiment. First, of course the source of GDNF ligand in vivo is the mesenchyme. The explant assay was designed to eliminate this and then to substitute GDNF as provided experimentally. The focus of the experiment was to address the response to GDNF, not the source of GDNF. But more importantly, the experiment

revealed a surprising outcome that the reviewer did not appreciate. In *Pax2Cre/Ret* mutants, the Wnt1Cre lineage still expresses Ret, yet does not grow out from the gut explant when provided with GDNF. This shows that the neural crest lineage requires Ret function in placode-derived cells in order to respond to GDNF. In other words, despite expressing Ret, the NC lineage does not harbor a cellautonomous response to GDNF, as we wrote. Because this might be confusing to some readers, we have revised the description of this analysis to hopefully be more clear.

> *(5) The fact that Ret and Ednrb signaling pathways interact is not a novel finding and has been reported multiple times in Ret and Ednrb mutant mice and cell lines (PMID: 12355085, 12574515 , 27693352, 31818953), potentially through shared transcription factors (PMID:31313802).It would have been more relevant if the authors could show how the specific tyrosine residue (Y 1015) in Ret is phosphorylated in the presence of Ednrb.*

The observation that human mutations in RET and EDNRB both cause Hirschsprung disease is decades old, and of course numerous studies in human, mouse, and cells have addressed the relation between the two signaling pathways. We did not mean to imply that we were the first to discover that Ret and Ednrb signaling pathways interact. The reviewer cites a number of papers all from the Chakravarti lab that address this phenomenon; while these are a valuable contribution to the field, there is still more to be learned. The model elaborated in PMID: 31313802, in which Ret and Ednrb are both enmeshed in a common gene regulatory network, does not readily explain why each has a different phenotypic manifestation and doesn't take into account the importance of the placodal lineage. The main new contributions of our paper are the existence of a new cell lineage that contributes to the ENS, and that the placodal and neural crest lineages utilize Ret and Ednrb signaling differently. The clarification of how these elements are differentially used by the two lineages explains long-segment and short-segment Hirschsprung disease (Ret and Ednrb mutants, respectively) far better than in past studies. The reviewer unfortunately dismisses these insights and seems to feel that a biochemical exploration of one specific component of the signaling interaction (Y1015 phosphorylation) would be more relevant. This should be the basis of future studies and are beyond the scope of the new findings reported in the present paper.

> *(6) What is the mechanism of the presence of Y1015 phosphorylation in 33% of Ednrb deficient Pax2Cre cells? It appears to me what the authors report as absent phosphorylation in the 67% of cells could be just weak staining or cells missing in prep.*

The reviewer, referring to Fig. 7q, presumably meant to say Wnt1Cre rather than Pax2Cre. The reviewer overlooked that we provided an explanation for this observation in our original manuscript. This sentence reads "Because Ednrb is expressed only in a subset of Wnt1Cre-derived enteric progenitor cells (Figure 7 – figure supplement 1), the residual Y1015 phosphorylation observed in Wnt1Cre/Ednrb mutant cells is likely to occur in the Ednrb-negative Wnt1Cre-derived cell population". The sentence is retained unchanged in the revised manuscript. The explanation is not because of weak staining or problems with tissue preparation.

> *(7) The references the authors cite regarding the previous discovery of Ret expression in the nucleus are incorrect. The review articles the authors cite do not mention anything about Ret expression in the nucleus. The evidence of nuclear localization of Ret previously comes from overexpression studies in HEK293 cells (PMID: 25795775). Such overexpression studies are fraught with generating noisy data for well-documented reasons. But if this observation is correct, the authors miss a great opportunity to identify what the Ret protein is doing in the nucleus. Is it in direct contact with its known*

> *transcription factors like Sox10 and Rarb? This would shed a lot of light on the possible mechanism of Ret LoF observed in Ret mutant mice*

The reviewer overlooked that the one of the review articles that we cited (Chen, Hsu, & Hung, 2020) has a dedicated paragraph for RET (section 3.14), which summarizes the work by Barheri-Yarmand et al (PMID: 25795775) which is the very paper noted by the reviewer in the comment above. The reviewer also somewhat misstated the results of the Barheri-Yarmand et al study. By immunostaining, this paper showed nuclear localization of endogenous Ret, albeit a version of Ret with a disease-associated mutation that makes it constitutively active by constitutive autophosphorylation. Nonetheless, this was endogenous Ret. The paper also used overexpression of GFP-tagged RET in HEK293 cells to show that wildtype RET can behave in a similar manner, at least under these circumstances. Our point is simply that Ret (and other receptor tyrosine kinases) can be found in the nucleus in certain biological contexts, and our observations are consistent with this precedent.

The reviewer also suggests a biochemical follow-up analysis related to this observation, which we agree would be of interest. Such an investigation however is beyond the scope of the present study.

> *(8) The manuscript could benefit from a major rewrite by reorganizing sections to make it easy for the readers to follow the narrative.*
>
> *Many sections about the role of Ret and Ednrb in Wnt1cre-derived ENCDCs can be moved to a supplement. These facts are well-documented and have been proven before.*

This was addressed in our response to comment #3 of this reviewer. The figures have been kept as main figures in the revised manuscript to allow side-by-side comparison to parallel analysis of the Pax2Cre lineage.

> *- The observation that only a handful of Pax2Cre cells at E10.5 express Ret and the observation that conditional Ret null abrogates these cells at E11.5, are not presented together and makes connecting these two facts difficult.*

Ret expression at E10.5 and E11.5 are both shown in the same figure (Fig. 2). In the presentation of these results, we first describe in normal development that Ret is expressed differently in E10.5 ENS progenitors between the Pax2Cre and Wnt1Cre lineages. This is additional support for the argument that the two lineages are molecularly distinct. Then comes evaluation of postnatal fates with different markers before we return to embryonic Ret expression. We acknowledge that this can make it difficult to connect these observations. We decided to retain the original organization in order to not lose this important conclusion. However, we have revised the text to hopefully make this connection between the sections more congruent.

> ***Reviewer #2 (Recommendations For The Authors**):*
>
> *- The labeling of some as "figure supplements" is really hard to follow in the text and confusing to interpret when a main figure or supplemental figure is being referenced, and which one.*

We understand this comment, but this is journal style and outside of our control. We have kept the journal format in the revised manuscript.

> *- The data in Figures 3b-c is well established in the field and somewhat misinterpreted. NOS1 neurons in the mouse ENS and their projections have been well described (Sang*

> *and Young, 1996, and other studies). CGRP immunoreactivity would reflect both ENS CGRP-expressing neurons and visceral afferents from DRG.*

There of course is a history of analysis of NOS1, CGRP, and other markers in the ENS. The focus of the analysis in Fig. 3 is to demonstrate how the cells that express these markers are impacted by gene manipulation in the Wnt1Cre and Pax2Cre lineages. For the giant migrating contractions that are associated with defecation, ample past electrophysiological studies have established that mechanosensory CGRP+ neurons trigger NOS+ inhibitory neurons (and ACh+ excitatory neurons) of the myenteric plexus to propel colonic contents. Thus, these are the relevant markers to explain the lack of colonic peristalsis in *Ednrb*-deficient mice. To our awareness, our results with NOS1 do not contradict any past study, including the Sang and Young 1996 description. Regarding CGRP, indeed the reviewer is correct that this marker is expressed by both neuronal subtypes. Two arguments support the specific derivation of ENS mechanosensory neurons from the Pax2 lineage. First, the ENS and DRG neurons can be distinguished by the location of their cell bodies and their axon extensions in the gut wall; only the ENS neurons are deficient in Pax2Cre/Ednrb mutants (as documented in Fig. 3). Second, the DRG population is derived from neural crest and is not labeled by Pax2Cre. If this population of CGRP+ neurons had functional relevance to colonic peristalsis, this would not be altered in Pax2Cre/Ednrb mutants. Indeed, the CGRP+ afferent nerve endings of DRG origin in the distal colon are mechanical distension sensors but do not modulate either ENS or autonomic nervous system activity (PMID: 37541195). We believe that our interpretation is correct.

> *- The evidence in Figure 3 supporting the claim that NOS1 and CGRP-expressing enteric neurons come from distinct lineages is weak. IHC for CGRP is notoriously poor at labeling soma in the ENS. IHC for tdTomato to ensure the detection of low levels of Tomato expression and quantification of observations would strengthen this claim.*

CGRP is a vesicular peptide which is stored and transported in vesicles, therefore the antibody against CGRP labels vesicular particles of soma and synaptic vesicles along the axons of those CGRP-producing neurons.

It is not expected to label the entire cytoplasm (or the range of subcellular organelles) as NOS antibody does. We did included quantification of data in Figure 3-figure supplement 1 in the manuscript to support the claim of lineage derivation. As described in the Methods section of the manuscript, we used binary threshold selection for Tomato+ cell count using Fiji-Image J, which detects both TomatoHigh and TomatoLow cells as Tomato+; we feel this is equal to or even superior to IHC for this analysis.

> *- IHC panels in Figures 3h-o are largely uninterpretable. Most of the signal seems to be non-specific background staining in the mucosa and quantification of mucosal signal in this context does not seem meaningful.*

We disagree with the reviewer's comment. As described in the response above, CGRP+ mechanosensory neurons send their peripheral axon projections to innervate mucosa (sensory epithelial cells), and NOS+ inhibitory motor axons innervate the circular muscle. Thus, panels h-o of Fig. 3 focus on the axonal profile and are not intended to visualize soma, which is why sagittal views are presented instead of flatmount views. All of the controls were performed side-by-side to confirm that the signal is real and interpretable.

> *Note also that the colon does not have villi so this annotation should be revised.*

We appreciate that the reviewer brought this misstatement to our attention. We corrected this error in the revised manuscript.

- Phospho-RET staining in Figure 7 is difficult to discern and interpret with high background. Positive and negative controls would strengthen these data.

Fig. 7 shows phospho Ret-Y1015 staining in lineage-labeled *Wnt1Cre/Ednrb/R26nTnG* mutants. The strength of the signal to noise in the figure is a matter of Ret expression level and the quality of the anti-pY1015 antibody. We are not aware of a meaningful positive control that has been validated in the literature that we could use for comparison. The ideal negative control would be to perform the same analysis in *Wnt1Cre/Ret/R26nTnG* mutants, but because this manipulation eliminates the entire NC cell lineage from the colon, there would be no NC cells in which to visualize background staining in this lineage with this antibody when Ret protein is not present. We note that anti-pY1096 did not show a difference in staining between control and mutant, which supports the interpretation of a specific impact on pY1015. We also point out here, as in the text, that we do not yet have any validation that phosphorylation of Y1015 is functionally important in NC migration to the distal colon. Clearly, more work to address this role and to demonstrate the mechanism of phosphorylation of this specific residue in response to Edn3-Ednrb signaling will be needed.

https://doi.org/10.7554/eLife.96424.2.sa0